RUPRECHT-KARLS-UNIVERSITÄT HEIDELBERG

Björn Gosdzik

Comparison of Calorimeter Signals with Trigger Signals at the ATLAS Experiment

Diploma Thesis

HD-KIP-07-03

KIRCHHOFF-INSTITUT FÜR PHYSIK

Faculty of Physics and Astronomy
University of Heidelberg

Diploma thesis
in Physics

submitted by
Björn Gosdzik
born in Bad Pyrmont
2007

Comparison of Calorimeter Signals with Trigger Signals at the ATLAS Experiment

This diploma thesis has bee carried out by Björn Gosdzik at the
Kirchhoff-Institut für Physik
under the supervision of
Prof. Dr. Karlheinz Meier

Abstract

This thesis describes the development of a software for the comparison of signals, recorded with the calorimeter with accordant signals of the Level-1 Calorimeter Trigger of the ATLAS experiment. Initial tests were accomplished and a fit function for the analysing of the signals was developed.

Signals recorded with the detector are digitized in the front-end electronic of the calorimeter, whereas the Level-1 Trigger receives the same analog signals via 70 m long cables. These analog signals are digitized by the PreProcessor. The cosmic run 2005 served as source for calorimeter signals. The signals were reconstructed from the raw data using the framework *Athena*. The trigger signals were generated by the charge injection system of the calorimeter and recorded via the VME readout of the PreProcessor. The developed software converts the different signals to the same format and compares them.

Initial test and comparison with the fit function demonstrates the alteration of analog trigger signals in pulse shape. Effects due to the influence of electronics and cables can be understood.

Zusammenfassung

Diese Arbeit beschreibt die Entwicklung einer Software zum Vergleich von Signalen, aufgenommen am Kalorimeter mit entsprechenden Signalen des Level-1 Kalorimeter Triggers des ATLAS Experiments. Erste Tests wurden durchgeführt und eine Fit-Funktion für die Analyse der Signale wurde entwickelt.

Während am Detektor aufgenommenen Signale in der Front-End Elektronik des Kalorimeters digitalisiert werden, empfängt der Level-1 Trigger dieselben analogen Signale über 70 m lange Kabel. Diese werden durch den PreProcessor digitalisiert. Als Quelle für Kalorimeter Signale diente der Cosmic Run 2005. Die Signale wurden aus Rohdaten mit Hilfe des Frameworks *Athena* rekonstruiert. Die Trigger Signale wurden mit dem Charge Injection System des Kalorimeters erzeugt und über den VME Readout des PreProcessors aufgenommen. Die entwickelte Software konvertiert die unterschiedlichen Signale in das selbe Format und vergleicht diese.

Erste Tests und Vergleiche mit Hilfe einer Fit-Funktion zeigen, dass sich die analogen Trigger Signale in ihrer Pulsform verändern. Die Effekte die durch den Einfluss von Elektronik und Kabel hervorgerufen werden können verstanden werden.

Contents

Chapter 1

Introduction

From the beginning of the 20th century particle physics made big progress. Starting with the detection of the three particles proton (p), neutron (n) and electron (e) building the atom more fundamental particles, e.g. the quarks were discovered and formed the theory of the Standard Model (SM). Many experimental data can be explained now but there are still open questions.

At the beginning of the 21st century the LHC and some of the four biggest detectors ever build are being constructed near Geneva to search for new phenomena beyond the SM. To realize the huge challenge of building the ATLAS detector a collaboration was formed, existing out of more than 150 institutes and laboratories in 35 countries including 1800 physicists.

One of the main goals of ATLAS is the detection of the Higgs boson which is expected within the Standard Model, and to search for new particles as a sign of new physics beyond the SM, e.g. the Minimal-Super-Symmetric-Standard Model (MSSM) as an expansion of the SM.

1.1 The Standard Model

The theory of the Standard Modell (SM) describes the fundamental particles and their interactions. Two different types of particles are known, fermions with spin 1/2 and bosons with spin 1. Leptons and quarks are spin 1/2 particles whereas the gauge bosons are spin 1 particles.

	1	2	3	charge
Quarks	u	c	t	$+\frac{2}{3}$
	d	s	b	$-\frac{1}{3}$
Leptons	e	μ	τ	-1
	ν_e	ν_μ	ν_τ	0

Table 1.1: Fermions in the SM

Both fermion families have three generations, each generation includes

2 particles. This leads to a total number of 12 fundamental particles as shown in Tab.1.1. Each of these 12 particles has its antiparticle so the SM consists totally out of 24 fundamental particles. Only 1/3 of these particles are responsible for the matter which surround us: up-quark (u) and down-quark (d) are building the inner structure of the proton (uud) and the neutron (udd) plus the first generation of leptons with the electron (e) and the associated electron-neutrino (ν_e). For a not yet understood reason there are two more generations.

Four different forces are known: the strong interaction, the electromagnetic interaction, the weak interaction and the gravitation, but only the first three are important for particle physics as the gravitation couples on mass and ranges over big distance but too weak for processes which appear in particle collisions. The forces are carried by the gauge bosons. For the weak interaction three bosons, the $W^{\pm}$ and the Z boson are responsible, the electromagnetic interaction is mediated by the photon (γ) and the strong interaction by 8 gluons (g), as shown in Tab. 1.2.

Interaction	**Boson**	**Coupling**	**Symmetry group**
weak	$W^{\pm}$ Z	weak charge	SU(2)
electromagnetic	Photon (γ)	el. charge	U(1)
strong	gluons (g)	colour	SU(3)

Table 1.2: Gauge bosons in the SM

The description of the fundamental particles and interactions is combined in the symmetry group of this theory, the $SU(3) \times SU(2) \times U(1)$. The left-handed states of the leptons and quarks are doublets under SU(2), while the right-handed states are singlets. With six quark flavors, the weak current is described by unitary transformations among the three quark doublets. The mixing between these three doublets describes the Cabibbo-Kobayashi-Maskawa matrix (CKM) [3], [4].

$SU(2) \times U(1)$ describes the so called electroweak interaction. This symmetry group is spontaneously broken by the Higgs field with non-zero expectation value. The higgs field would be responsible for the mass of the vector bosons, the W and the Z, while the photon remains massless.

The group SU(3) describes quantum chromodynamics (QCD). Under this group quarks are also triplets as they are carrying an additional charge, called colour. The gauge bosons of SU(3) are gluons which are carrying colour, too and therefore they are also self-interacting.

The Standard Model has in its simplest version 19 free parameters from which 17 are known with varying errors. These parameters are the three coupling constants of $SU(3) \times SU(2) \times U(1)$, three lepton and six quark masses, the mass of the Z boson which sets the scale of weak interactions and the four parameters describing the rotation from the weak to the mass

eigenstates of the quarks (CKM matrix). One of the two remaining parameters is the CP-violating parameter for strong interactions which must be very small, the last parameter is associated with the mechanism which is responsible for the breakdown of the SU(2) × U(1). This could be the mass of the not yet discovered Higgs boson, a neutral scalar boson H^0. The search for the Higgs is one of the main goals of ATLAS.

1.2 pp-physics at LHC

The high energy and high luminosity available to the ATLAS experiment will offer a large range of physics opportunities. Both the precise measurement of properties of known objects and the discovery of new physics will be possible. The main goal is the full understanding of the SM by the detection of the Higgs boson but there are many other important goals, too. The search for super-symmetric particles, new gauge bosons and composite quarks and leptons, the investigation of CP violation in B decays and the precise measurement of the W mass and the top-quark decay.

1.2.1 pp interactions

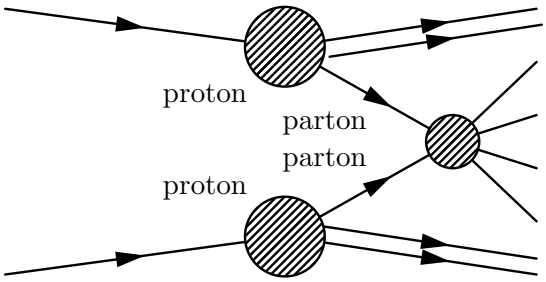

Figure 1.1: Feynman diagram of a parton-parton interaction in a pp-collision at LHC

During a proton-proton head-on collision several hadrons are produced and build jets. The interactions of protons can be described as interactions of their constituent partons. As shown in Fig. 1.1 one quark of each proton takes part in the collision, whereas the other partons are so-called spectator quarks. The cross section for parton-parton interactions can be described as:

$$\sigma = \int f_1(x_1, Q^2) f_2(x_2, Q^2) \sigma_{parton}(x_1, x_2, Q)$$

The calculation of the production cross section at the LHC for interesting physics processes and their backgrounds relies upon the knowledge of the distribution of the momentum fraction x of the partons in a proton. These parton distribution functions (PDFs) are provided by two major groups,

CTEQ and MRS. The PDFs are determined by global fits to data from deep inelastic scattering, Drell-Yan, jets and direct photon production at current energies. The newest PDFs provide the most accurate description of the world's data. In Fig. 1.2 the newest parton distribution from the CTEQ group is shown with an momentum transfer Q=100 GeV.

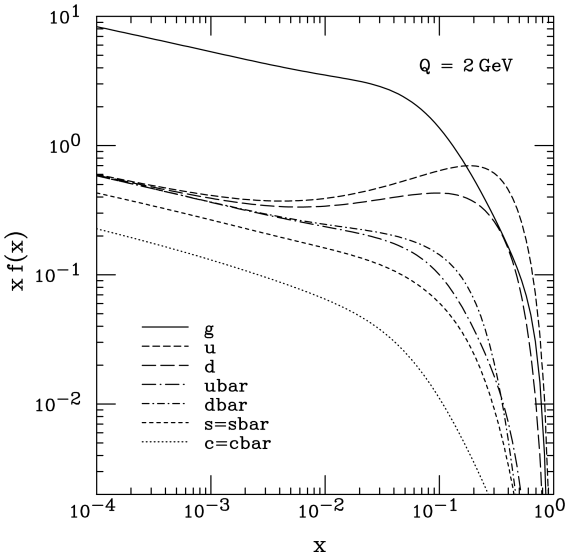

Figure 1.2: Parton distribution for the CTEQ6M PDF at Q=100 GeV [2]

1.2.2 The Higgs boson

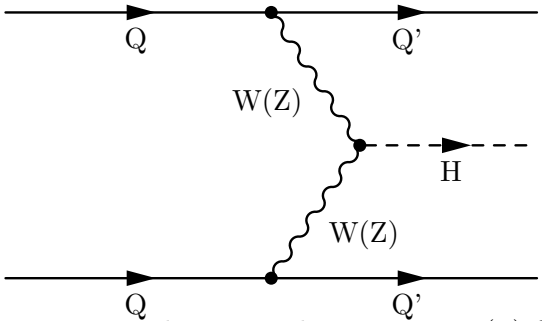

Figure 1.3: Higgs boson production in a W(Z) fusion

For a better understanding of the electroweak symmetry-breaking the observation of one or several Higgs bosons will be fundamental. The Standard Model assumes a doublet of scalar fields. This demands the existence of one neutral scalar particle, the Higgs boson H. An upper limit of ∼1 TeV can be derived. From experimental results a Higgs mass of $m_H < 114.3$ GeV can be excluded.

For SUSY the Higgs sector is extended to at least two doublets of scalar fields. This results in five particles in the minimal version of super-symmetry the MSSM: two CP-even Higgs bosons h and H, one CP-odd boson A and two charged Higgs $H^{\pm}$.

Boson	**Mass**	**CL**
H	$m_H > 114.3$ GeV	95%
h	$m_h > 89.8$ GeV	95%
A	$m_A > 90.1$ GeV	95%
$H^{\pm}$	$m_{H^{\pm}} > 79.3$ GeV	95%

Table 1.3: Mass of Higgs bosons. The limits are obtained from the four LEP experiments ALEPH, DELPHI, L3 and OPAL.

The production of the Higgs Boson in the SM is dominated by the gg fusion and the WW fusion but also the $q\overline{q}$ and ZZ fusion contribute to the total cross-section. A Feynman diagram of higgs boson production in W(Z) fusion is shown in Fig. 1.3. The W bosons are emitted from incoming quarks. Due to the high fraction of $\sigma_{parton}(x_1, x_2, Q)$ the cross section of this process is also high. For its discovery the SM Higgs boson is searched in various decay channels at the LHC. These channels are:

- $H \rightarrow \gamma\gamma$ direct production
- $H \rightarrow \gamma\gamma$ from the associated production WH, ZH and $t\overline{t}H$
- $H \rightarrow b\overline{b}$ from the associated production WH, ZH and $t\overline{t}H$
- $H \rightarrow ZZ \rightarrow 4l$
- $H \rightarrow ZZ \rightarrow 4l$ and $H \rightarrow ZZ \rightarrow ll\nu\nu$
- $H \rightarrow WW \rightarrow l\nu jj$ and $H \rightarrow ZZ \rightarrow lljj$

Over the full mass range up to ≈1 TeV a Standard Model Higgs can be discovered in ATLAS with a high significance. A 5σ-discovery can be achieved within a few years running at low luminosity, which is 1/10 less than design luminosity. To cover the full mass range and to achieve the 5σ-significance it is essential to look on as many channels as possible. Fig. 1.4 (a) shows the significance for every channel mentioned above and the total significance of all of these channels, the sensitivity for the discovery of MSSM Higgs bosons is shown in Fig. 1.4 (b).

In case of a discovery with an integrated luminosity of 300 fb^{-1} the mass would be measured with a precision of 0.1% over the mass range of 80 - 400 GeV, the width with a precision of 6% over a mass range of 300 - 700 GeV, the Higgs production rate with 10% and the most important couplings and branching ration with a precision of the order of 25%. Precise measurements

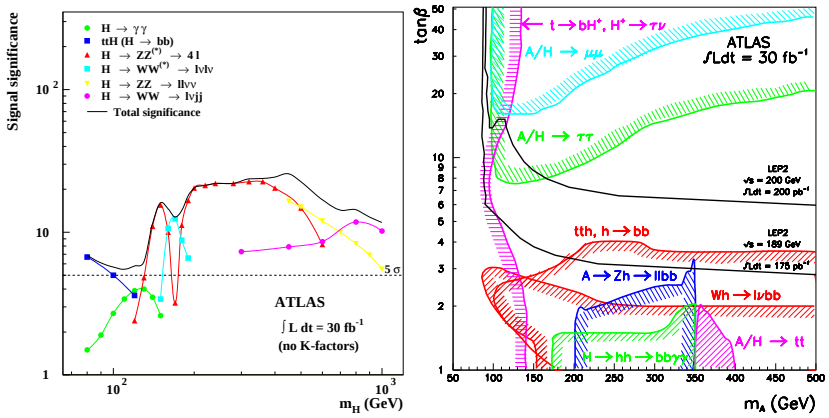

(a) (b)

Figure 1.4: ATLAS sensitivity for the discovery of a Standard Model Higgs boson (a) and of MSSM Higgs bosons (b) [9]

of these parameters and measurements of other properties like spin and self-coupling will be possible by the International Linear Collider (ILC).

1.2.3 Supersymmetry

Name	Spin 1/2	Spin 1
gluino, gluon	$\tilde{g}$	g
winos, W's	$\tilde{W}^{\pm}, \tilde{W}^{0}$	$W^{\pm}, W^{0}$
bino, B	$\tilde{B}$	B

Table 1.4: Vector supermultiplets in the MSSM

If SUSY exist at the weak scale, M ≈1 TeV, then supersymmetric particles will be discovered at the LHC. ATLAS can make precise measurements of SUSY masses and use them to infer properties of the underlying SUSY model.

The MSSM is the Minimal Supersymmetric extension of the Standard Model. In the MSSM each chiral fermion $f_{L,R}$ has a scalar sfermion partner $\tilde{f}_{L,R}$ and each massless gauge boson A_{μ} with two helicity states ±1 has a massless spin-1/2 gaugino partner with helicity ±1/2. The complete list of all particles are shown in Tab. 1.4 and Tab. 1.5.

Name	Spin 0	Spin 1/2
squarks, quarks	$\tilde{Q} = (\tilde{u}_L, \tilde{d}_L)$	$Q = (u_L, d_L)$
	$\tilde{u}_R$	$\bar{u}_r$
	$\tilde{d}_R$	$\bar{d}_r$
sleptons, leptons	$\tilde{L} = (\tilde{\nu}, \tilde{e}_L)$	$L = (\nu, e_L)$
	$\tilde{e}_R$	$\bar{e}_R$
Higgs, Higgsinos	$H_u = (H_u^+, H_u^0)$	$\tilde{H}_u = (\tilde{H}_u^+, \tilde{H}_u^0)$
	$H_d = (H_d^0, H_d^-)$	$\tilde{H}_d = (\tilde{H}_d^0, \tilde{H}_d^-)$

Table 1.5: Chiral supermultiplets in the MSSM

1.2.4 Compositeness

The large number of quarks and leptons led to the speculation that they have a substructure, i.e. they are bound states of more fundamentel constituents [5]. This mechanism is called compositeness.

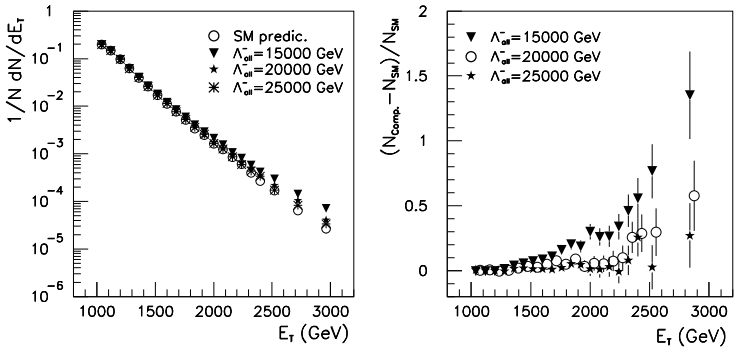

(a) (b)

Figure 1.5: E_T distribution for two leading jets, SM prediction (open circles) and effect of quark compositeness at 30 fb^{-1} of integrated luminosity (a), and difference of SM prediction and effect of compositeness on jet E_T distribution, normalized to SM rate with errors correspond to 30 fb^{-1} (b) [9]

The evidence of such a substructure can be observed by deviations from QCD predictions of jet rates, which will reveal new physics such as quark compositeness and the existence of other new particles. Essential tests of QCD are the measurement of the inclusive jet cross section and the study of the di-jet mass spectrum and angular distribution. The existence of a

quark substructure would appear as an excess event of high p_T compared to that predicted by QCD or as di-jet angular distributions that are more isotropic than that expected in a point-like quark theory. So far no evidence of quark substructure was found in other experiments such as CDF and D0 at a center-of-mass energy of 1.8 TeV.

The effect of compositeness on the inclusive jet energy spectrum for an integrated luminosities of 30 fb^{-1} and different compositeness scales Λ is shown in Fig. 1.5. This effect could be masked by the uncertainties of the parton distribution functions (PDFs). More sensitive to compositeness than the jet E_T spectrum and less sensitive to the non-linearity of the calorimeter is the angular distribution of the jets. The di-jet angular distribution for di-jets and different compositeness scales Λ is $(1/N)(dN/d\chi)$, where $\chi \equiv e^{|\eta_1-\eta_2|}$ with $\eta_{1,2}$ as the pseudorapidities of the two leading jets. The high mass di-jet angular distribution has an excellent discovery capability for quark compositeness. If the constituent intercation constant is of the order of 14 TeV the quark substructure can be discovered within one month of LHC operation at $10^{33}cm^{-2}s^{-1}$. To reach a 95% CL limit of 40 TeV an integrated luminosity of 300 fb^{-1} is needed.

Chapter 2

The ATLAS Experiment and the LHC

2.1 The Large Hadron Collider at CERN

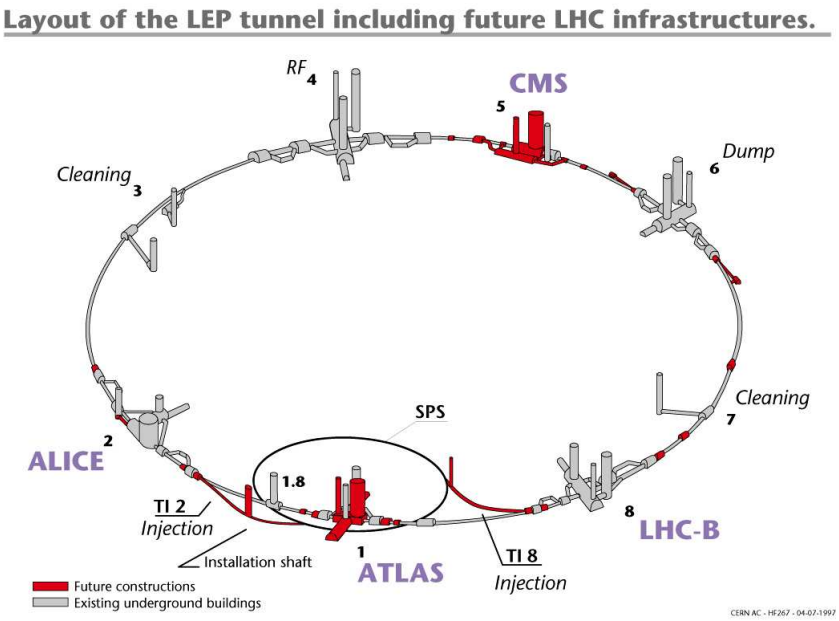

Figure 2.1: Layout of the LHC [14]

The Large Hadron Collider (LHC) is a particle accelerator, which is currently being build in the former LEP tunnel at CERN. First collision are planned for November 2007. The layout of the collider is shown in Fig. 2.1. It will bring protons as well as heavy-ions (e.g. Pb) to head-on collisions.

The goal of the LHC is the discovery of the Higgs boson and the study of rare physics at a center-of-mass energy of $\sqrt{s} = 14$ TeV and at very

high luminosity of L = 10^{34}cm^{-2}s^{-1}. The experiments ALICE[1], ATLAS[2], CMS[3] and LHCb[4] are currently being build at the four collision points of the LHC. The accelerator has 8 straight sections connected by 8 arcs and a circumference of about 26.7 km. The two experiments focused on pp interactions, ATLAS (IP1)[5] and CMS(IP5), are located in diametrically opposite straight sections as shown in Fig. 2.1.

The LHC is designed to produce a very high number of events. To perform this unprecedented requirement of event number the collider has a very high luminosity. The number of events per second is given by:

$$N_{event} = L\sigma_{process}$$

where σ_{process} is the cross section for a certain process and L the luminosity of the machine. The luminosity is given by:

$$L = \frac{N_b^2 n_b f_{rev} \gamma_r}{4\pi\epsilon_n \beta^*} F$$

with N_b as the number of particles per bunch, n_b the number of bunches, f_{rev} the revolution frequency, γ_r the relativistic gamma factor, ϵ_n the normalized transverse beam emittance, β^* the beta function at the collision point and F the geometric luminosity reduction factor due to the crossing angle at the IP. The high beam energy and the high beam intensity are the requirements for the exploration of rare events. A very high rapidity and high trigger rate are the demands on the trigger due to the large number of events.

With each filling the collider will be filled with 2808 bunches, each bunch contains 10^{11} protons. The protons are injected at an energy of 450 GeV and accelerated to the final energy of 7000 GeV. In a storage ring the peak beam energy depends on the integrated dipole field along the ring circumference. The energy of 7 TeV implies a peak dipole field of 8.33 T. The RMS bunch length is 7.55 cm and the RMS beam size at IP1 and IP5 is 16.7 μm. With a bunch crossing rate of about 40 MHz about 23 collisions take place every 25 ns.

2.2 The ATLAS Detector

The ATLAS Detector is one of the two main experiments at the LHC. Its main goal is to operate at a high luminosity (10^{34}cm^{-2}s^{-1}) to provide as many interesting events as possible using electron, gamma, muon, jets and

[1] **A** **L**arge **I**on **C**ollider **E**xperiment
[2] **A** **T**oroidal **L**HC **A**pparatu**S**
[3] **C**ompact **M**uon **S**olenoid
[4] **L**arge **H**adron **C**ollider **b**eauty
[5] **I**nteraction **P**oint

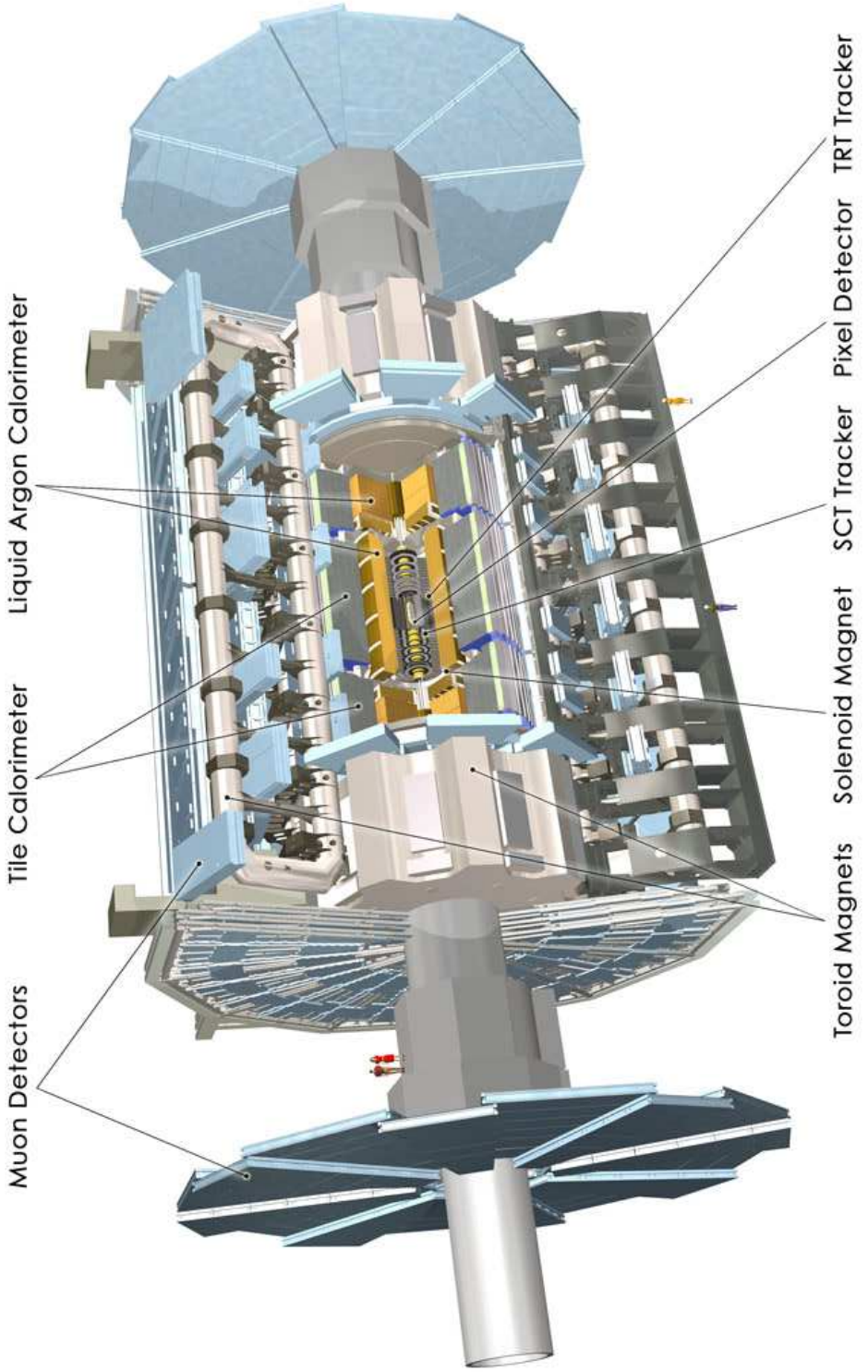

Figure 2.2: The ATLAS Detector [14]

measurements of missing transverse energy. The basic design criteria for the detector are:

- Efficient tracking at high luminosity for high-p_T lepton-momentum measurements, electron and photon identification, τ-lepton and heavy-flavor identification and full event reconstruction capability at lower luminosity
- Very good electromagnetic calorimeter for electron and photon detection and measurements with an excellent energy resolution over the range of 10 - 300 GeV
- A full coverage hadronic calorimeter for measurements of jets and missing transverse energy (E_T^{miss}) covering the range of $|\eta| \approx 5$ for allowing an efficient tagging of forward jets
- High-precision measurements of muon momentum with a resolution $\frac{\Delta p_T}{p_T} \sim 10\%$
- Large acceptance in pseudorapidity (η) with almost full azimuthal angle (ϕ) coverage everywhere. The azimuthal angle is measured around the beam axis, whereas pseudorapidity relates to the polar angle (θ) where θ is the angle from the z direction.
- Triggering and measurements of particles at low-p_T thresholds, providing high efficiencies for most physics processes of interest at LHC

The layout of the detector includes the Inner Detector (ID) surrounded by a superconducting solenoid, a liquid argon (LAr) electromagnetic (EM) sampling calorimeter and a hadronic calorimeter, provided by a novel scinti llator-tile calorimeter (TileCal), large superconducting air-core toroids outside the calorimeters and a muon spectrometer which defines the overall dimension of the ATLAS detector. The length is 46 m, the diameter is 22 m and the overall weight of ATLAS is about 7000 tons. The beam direction defines the z-axis and the x-y-plane is the plane transverse to the z-axis. The positive x-axis is pointing from the interaction point to the center of the LHC ring, the positive y-axis is pointing upwards. The azimuthal angle (ϕ) is measured around the beam axis and the polar angle (θ) is the angle from the beam axis. In the ATLAS coordinate system the pseudorapidity is used which is defined as $\eta = -\ln\tan(\frac{\theta}{2})$. The tranverse momentum p_T and the transverse energy E_T as well as the missing transverse energy E_T^{miss} are defined in the x-y-plane. The distance ΔR in the pseudorapidity-azimuthal angle space is defined as $\Delta R = \sqrt{\Delta\eta^2 + \Delta\phi^2}$.

2.2.1 Inner Detector

The Inner Detector (ID) is a combination of high-resolution detectors at the inner radii and continuous tracking elements at the other radii, all contained

in the Central Solenoid (CS) with a nominal magnetic field of 2 T. The challenge of the ID is the measurement of the momentum and vertex with a high resolution. This high-precision measurements have to be made with very fine granularity detectors. To achieve this at the very large tracking density expected at LHC, semiconductor tracking detectors, using silicon microstrip and pixel technologies are used over a full tracking coverage of $|\eta| \leq 2.5$. The ID allows measurements of impact parameter and vertexing for heavy-flavor and τ tagging.

Pixel Detector

The pixel detector is designed to provide a very high granularity and a very high precision set of measurements as close to the intercation point as possible. It determines the impact parameter resolution and the ability of the ID to find short-lived particles such as B hadrons and τ leptons. The pixel detector contains a total of 140 million readout channels, each 50 μm in the $\mathrm{R} - \phi$ direction and 300 μm in the z direction. The system consist of three barrels at average radii of about 4 cm, 10 cm and 13 cm and five disk on each side, between radii of 11 cm and 20 cm covering $|\eta| = 1.7 - 2.5$.

Semiconductor Tracker

The Semiconductor Tracker (SCT) system is designed to provide eight precision measurements per track in the intermediate radial range. These measurements contribute to the measurement of momentum, impact parameter and vertex position, as well as providing good pattern recognition by the use of high granularity. The SCT contains 61 m^2 of silicon detectors, with a total of 6.2 million readout channels. The spatial resolution of each channel is 16 μm in $\mathrm{R} - \phi$ and 580 μm in z direction.

Transition Radiation Tracker

To operate at the very high rate expected at the LHC the Transition Radiation Tracker (TRT) is based on the use of straw tubes, which can operate on the needed rate due to the small diameter of the straws. Electron identification cability is added by employing xenon gas to detect transition-radiation photons created in a radiator between the straws. Each straw is 4 mm in diameter and equipped with a 30 μm diameter gold-plated W-Re wire, giving a fast response. The maximum length in the barrel is 144 cm. The barrel contains about 50 000 straws, the end-caps contains 320 000 radial straws. The total number of electronic channels is 370 000 with a spatial resolutions of 170 μm per straw. The TRT is operated with a non-flammable gas mixture of 70% Xe, 20% CO_2 and 10% CF_4.

2.2.2 LAr and Tile Calorimeter

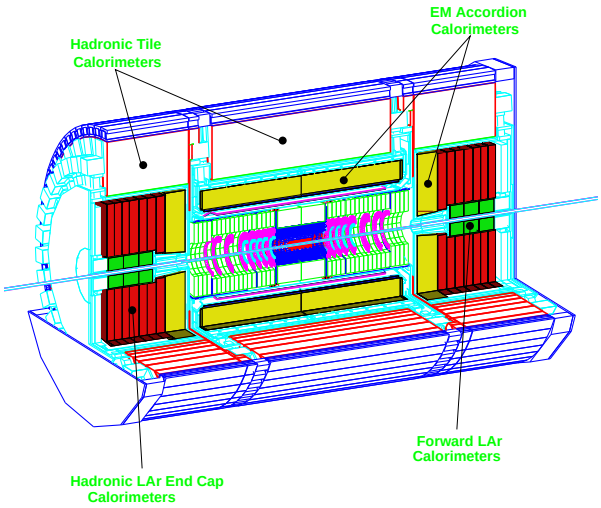

Figure 2.3: ATLAS Calorimeter [9]

The ATLAS calorimeter consist of several parts: an electromagnetic calorimeter (EC), a presampler, a hadronic tile calorimeter (TileCal), the hadronic end-cap calorimeter (HEC) and the forward calorimeter (FCAL). A schematic overview of the calorimeter is shown in Fig. 2.3 and the pseudorapidity coverage of the calorimeters is given in Tab. 2.1.

The EM is a lead/liquid-argon (LAr) calorimeter with accordion structure and preceded with a presampler detector to correct the energy lost in the material (Inner Detector, cryostat, coil). The TileCal is divided into three cylindrical sections: the central barrel and two identical extended barrels. These three sections are using sampling technique with plastic scintillator plates (tiles) and iron as absorber. For the calorimeters in larger pseudorapidities the intrinsically radiation-hard LAr technology is used since material in the forward region is exposed to a higher radiation: the hadronic end-cap calorimeter as a LAr detector with copper as passive material and the forward calorimeter, a dense LAr calorimeter with electrodes in a tungsten matrix.

Liquid Argon Calorimeter

The LAr sampling technique is radiation resistant and provides long-term stability of the detector response, a good energy resolution and relatively

Presample	**Barrel**	**End-Cap**
	$\|\eta\| < 1.52$	$1.5 < \|\eta\| < 1.8$
EM Calorimeter	**Barrel**	**End-Cap**
	$\|\eta\| < 1.475$	$1.375 < \|\eta\| < 3.2$
Hadronic Tile	**Barrel**	**Extended Barrel**
	$\|\eta\| < 1.0$	$0.8 < \|\eta\| < 1.7$
Hadronic LAr		**End-Cap**
		$1.5 < \|\eta\| < 3.2$
Forward Calorimeter		**Forward**
		$3.1 < \|\eta\| < 4.9$

Table 2.1: Pseudorapidity coverage of the calorimeters

easy detector calibration. It is used for the EM and the presampler, but due to the radiation resistance the LAr technique is also used for the HEC and the FCAL. For all these calorimeters liquid argon is the active material.

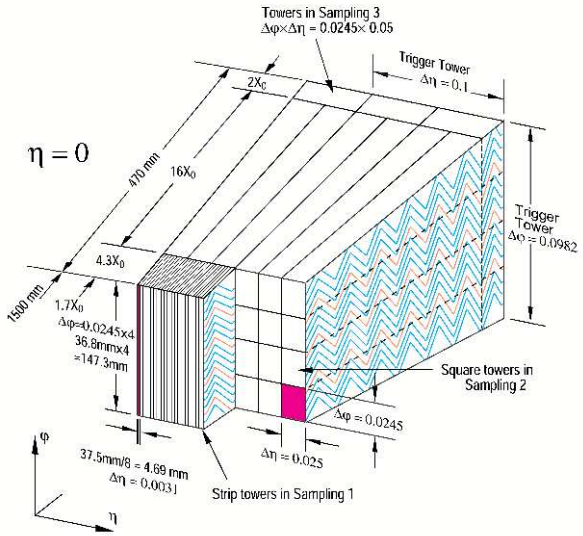

Figure 2.4: Design of the EM calorimeter [11]

The absorber material for the EM part are lead plates. The calorimeter is build as a accordion-shaped structure with Kapton electrodes, as shown in Fig. 2.4. This geometry provides complete ϕ symmetry without azimuthal

cracks. The total thickness of the calorimeter is > 24 radiation lengths (X_0) in the barrel and > 26 X_0 in the two end-caps.

The signals from about 190 000 channels are extracted at the inner and the outer faces and send to preamplifiers. After a Level-1 Accept, the corresponding samples (maximum 15 samples) are extracted, digitized and read out using Data ACquisition system (DAC). One sample corresponds to one bunch-crossing with a length of 25 ns.

HEC and FCAL are integrated in the same cryostat that is housing the EM end-cap. The absorber material for the hadronic end-cap are copper plates of different thickness. Hence iron, which is used in the TileCal, would distort the homogenous solenoid field, copper was chosen as a non-magnetic material but similar in terms of nuclear properties.

Located next to the region of incoming and outcoming beams the FCAL makes high demands on its design. To cope the high level of radiation in the forward region of the detector the FCAL consists of copper and tungsten, which is very resistant against radiation.

Tile Calorimeter

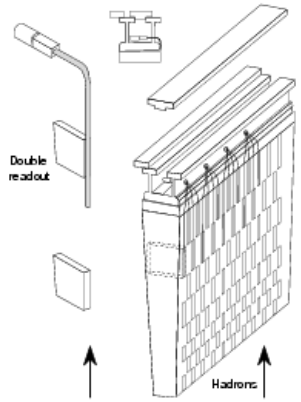

Figure 2.5: Design of the TileCal [11]

The barrel and the extended barrel of the hadronic calorimeter are using the iron scintillator-tile technique. Its design is shown in Fig. 2.5. The absorber material is iron while the active material are scintillating tiles. Two sides of each tile are read out by wavelength shifting fibres (WLS) into two separate photomultiplier tubes (PMTs). The inner radius of the tile calorimeter is 2.28m and the outer radius is 4.25 m. Longitudinally it is segmented into three layers, 1.4, 4.0 and 1.8 interaction lengths thick at $\eta = 0$. Azimuthally the barrel and extended barrel are divided into 64 modules. The granularity of the TileCal is $\Delta\eta \times \Delta\phi = 0.1 \times 0.1$ (0.2×0.1 in the last layer) and it has about 10 000 read out channels.

An important parameter of the calorimeter is its thickness: to provide good containment for hadronic showers and to reduce punch-through of high energetic particles into the muon system to a minimum, the total thickness is 11 interaction length (λ) at $\eta = 0$. Since 10 λ of active calorimeter provide a good resolution for high energy jets and together with the large $\eta-$coverage, this will guarantee a good E_T^{miss} measurement, which is very important for many physics signatures.

2.2.3 Muon Spectrometer

The concept of the muon system is based on the deflection of muon tracks in superconducting air-core toroid magnets. This deflection is provided by a magnetic field. The tracks are measured in three chambers arranged cylindrical around the beam axis. In the transition and end-cap regions this chambers are installed vertically, also in three layers. In most of the region measurements are done by Monitored Drift Tubes (MDT) while in the forward region and close to the interaction point this is realized by Cathode Strip Chambers (CSCs).

2.2.4 Magnet system

The ATLAS superconducting magnetic system consists of a central solenoid (CS) for the Inner Detector magnetic field and three large air-core toroids generating the magnetic field for the muon spectrometer. The two end-cap toroids (ECT) are lined up with the CS at each end and are inserted in the barrel toroid (BT).

The central field of the CS is 2 T with a peak field of 2.6 T at the superconductor itself. The peak field of the BT and ECT are 3.9 T and 4.1 T respectively. The CS coil is as thin as possible while the three toroids consist of eight huge coils assembled radially and symmetrically around the beam axis.

The magnets are indirectly cooled by forced flow of helium at 4.5 K. Whereas the CS is powered by 8 kA power supplies, the toroid coil is equipped with 21 kA power suplies. Both the 8 coils of the BT and the 16 coils in the two ECTs are connected in series.

Chapter 3

The ATLAS Trigger System

3.1 Trigger overview

The task of the ATLAS trigger system is to select rare, interesting physics events with a high efficiency while rejecting a much higher-rate of background events. Managing this operation with a rate of 10^9 interactions per second is the main challenge. Since the LHC has a bunch-crossing rate of 40 MHz every 25 ns decisions must be made whether a certain event is taken or not. At high luminosity 23 inelastic pp-interactions take place in each bunch-crossing. The average event size is about 1.6 Mbyte. The goal is to achieve a storage rate of approximately 200 Hz to reduce data volume.

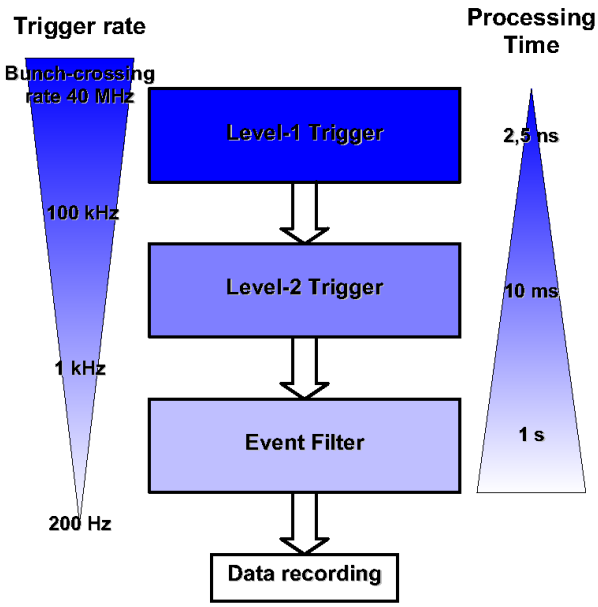

Figure 3.1: Block diagram of the Trigger/DAQ system [7]

The ATLAS trigger consists of three physical layers: the Level 1 trigger (LVL1), Level 2 trigger (LVL2) and the Event Filter (EF). A schematic overview on all three layers is shown in Fig. 3.1.

The LVL1 trigger has access to the whole calorimeter system and the muon spectrometer on a reduced granularity and receives data at the full LHC bunch-crossing rate of 40 MHz. The output rate is 75 kHz (upgradable to 100 kHz). While the LVL1 trigger is forming the trigger decision, the information of all detector channels are stored in so-called "pipeline" memories. In case of a positive decision the selected event is read out from the front-end electronics close to the detector into readout buffers (ROBs). As a compromise of cost and performance the pipeline length is kept as short as possible. Therefore the latency of the LVL1 trigger, measured from the time of collision until trigger decision taken, is 2 μs plus 500 ns contingency.

The LVL1 trigger provides regions of interest (RoI) for the LVL2 trigger. These regions include information on the position (η and ϕ coordinates), p_t of candidates and the energy sums. The LVL2 triggers is focused only on the RoIs but with the full detector informations available.

While the Level-1 trigger is a pure hardware system, the Level-2 trigger as well as the Event Filter are using PC farms on which dedicated algorithms are running. The LVL2 reduces the rate to $\approx$ 1 kHz while the latency can vary from event to event.

The algorithms of the EF is based on offline code and reduces the rate to $\approx$ 100 Hz. Events accepted by this level are stored.

3.2 The Trigger System

3.2.1 The Level-1 Trigger

The LVL1 trigger receives data/signals from the muon trigger chambers and the calorimeters. Running at the bunch-crossing rate of 40 MHz it is build as a synchronous, pipelined hardware system. The clock is synchronized by the LHC machine clock which is adjusted to the bunch-crossing rate. Additional to the bunch-crossing signal a bunch-zero signal is received once per turn every 88 μs.

The trigger forms its decision on the following trigger objects:

- muon
- e.m. clusters
- narrow jets (isolated hadronic tau decays or isolated single hadrons)
- jets
- missing transverse energy

- total scalar transverse energy

As shown in Fig. 3.2 the LVL1 trigger has several components: the calorimeter trigger with submodules, the muon trigger with submodules, the Central Trigger Processor (CTP) and the Timing, Trigger and Control (TTC). Whereas the CTP is generating the trigger decision (Level1-Accept for a positive decision) based on the information from the calorimeter trigger and the muon trigger the TTC is responsible for providing this decision to the front-end and readout systems of all ATLAS subsystems.

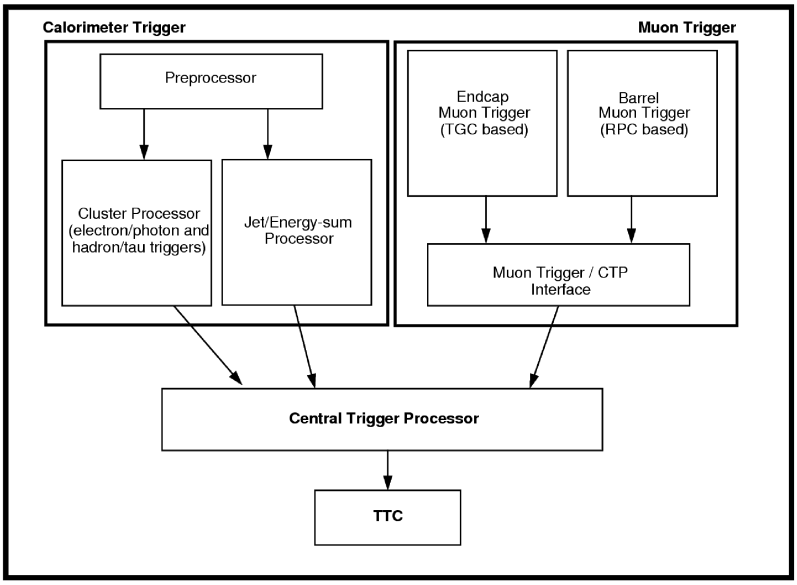

Figure 3.2: Block diagram of the LVL1 trigger [6]

3.2.2 The High Level Trigger (HLT)

The HLT consists of two components: the Level-2 trigger and the Event Filter. Both are build using farms of standard PCs interconnected by networks. The LVL2 has to manage the output rate of the LVL1 trigger and has an average latency of ≈10 ms. Having access to the full detector granularity the second trigger level will only use a fraction (typically ≈2%) of event data based on RoIs. RoIs are Regions of Interests found by the LVL1 trigger. The LVL2 trigger is using a sequence of highly optimized trigger selection algorithms guided by the RoIs. For example em-cluster or em-cluster plus isolated tracks.

Being the third an last stage of the online selection chain the EF is using the offline framework *ATHENA* and the Event Selection Software. The EF has to work on the LVL2 accept rate with an average event treatment time of ≈1 s.

3.3 The Level-1 Calorimeter Trigger

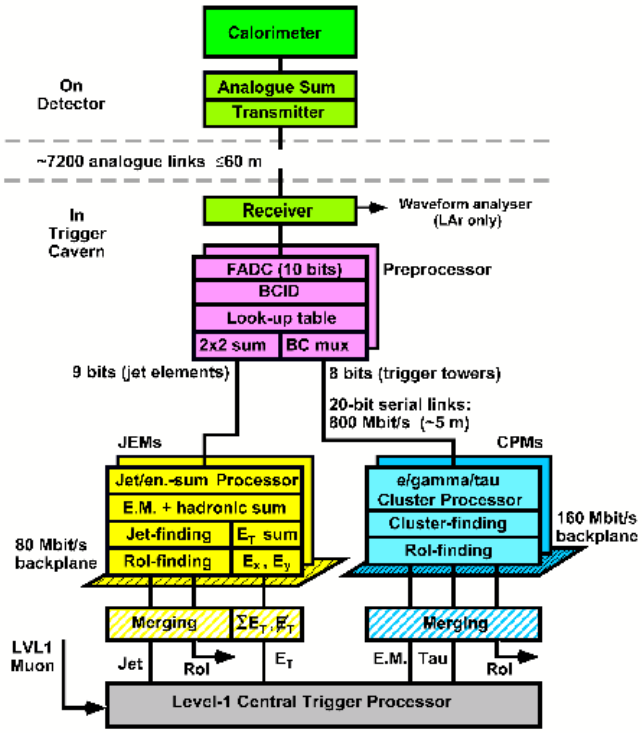

Figure 3.3: Architecture of the LVL1 trigger [6]

The Level-1 Calorimeter Trigger is split up in three parts: the PreProcessor (PPr), the Cluster Processor (CP) and the Jet/Energy-sum Processor (JEP). The full system is build in racks, each rack housing two crates and is located in the electronic cave USA15. The architecture of the calorimeter trigger is shown in Fig. 3.3.

The real time analog signals are received by receivers, located next to the PreProcessor system to guarantee a cable length as short as possible due to the latency of 2 μs. A trigger tower signal covers the range of 0 to 2.5 V corresponding to a transverse energy from 0 to 250 GeV. Pulses with a larger energy deposition are saturated.

3.3.1 PreProcessor

The PreProcessor receives ≈7200 analog signals from the electromagnetic and the hadronic calorimeter. Originally from about 200 000 channels a coarser granularity is used for the trigger to obtain this small number of signals. Therefore trigger tower signals are formed by summing the finer granularity cell signals within the calorimeter front-end electronics. The

granularity of a trigger tower is about $\Delta\eta \times \Delta\phi = 0.1 \times 0.1$, for $|\eta| > 2.5$ the tower size is changing to large values, and for $|\eta| > 3.2$ the tower definition becomes more complicated.

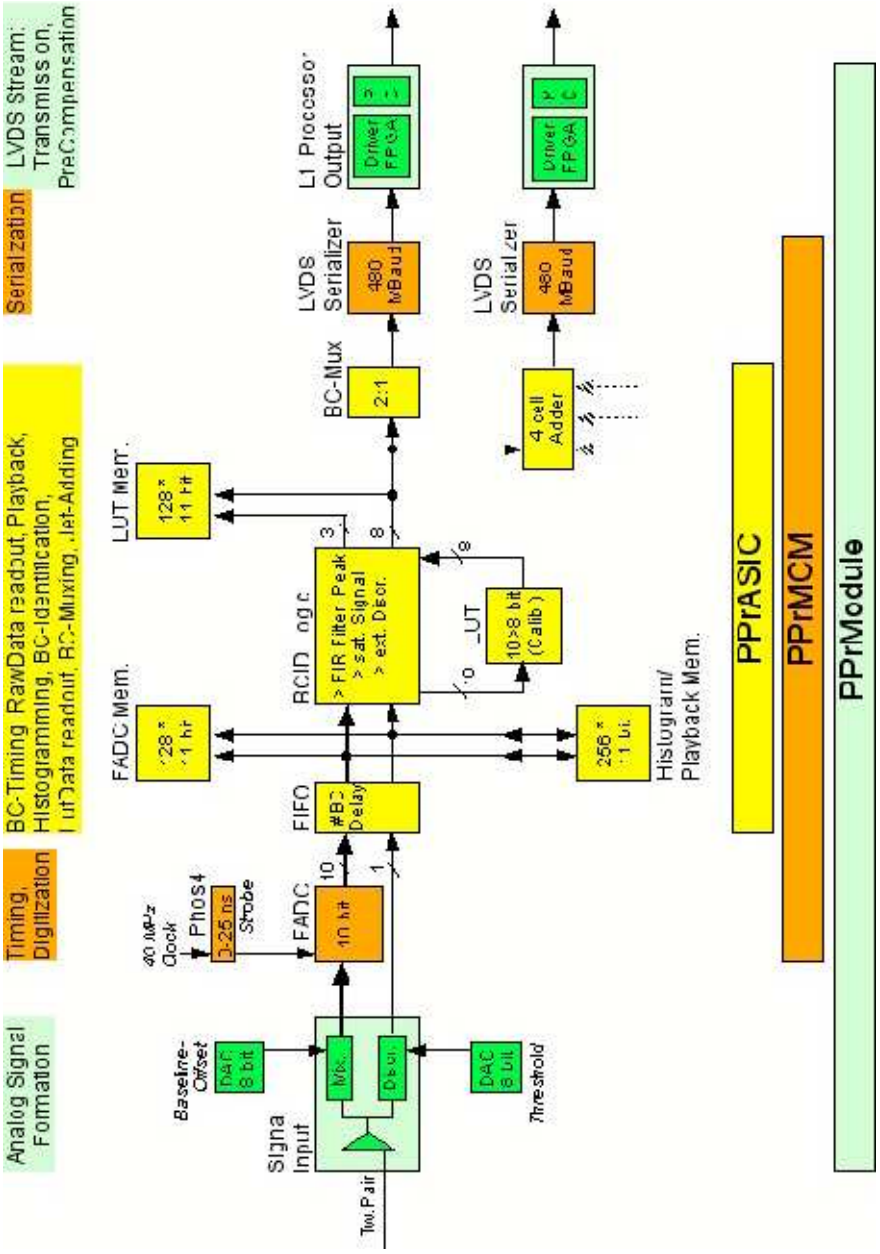

Figure 3.4: Block diagram of processing of one trigger channel [15]

The total PreProcessor system is housed in 8 crates separated in 4 racks. Two racks on side A, respectively side C. Six crates contain 16 PreProcessor

Modules (PPMs) and two crates are equipped with 14 PPMs leading to a total number of 124 modules. Some additional modules important for the operation of the system reside in each crate, not only for the PPr but also for the CP and the JEP:

- A Timing and Control Module (TCM) receives and distributes the TTC protocol. This protocol includes the LHC-clock, L1-Accept, synchronizing reset and broadcast for system synchronization
- A network connected CPU acts as a local controller of the VME Bus
- A G-Link board for each PPM for transmission of DAQ-data to the ReadOut Driver Module (ROD)

The trigger logic is build upon ϕ quadrants. Two racks cover the +z-side, the -z-side is mirror-symmetric. Both, PPMs for the electromagentic calorimeter and for the hadronic calorimeter are identical in hardware. Each PPM processes 64 channels on one 9U VME64xP board. Four cables are plugged in on the front-panel of the module, each cable is carrying 16 signals. The processing chain (the so-called real-time path) of one single channel is shown in Fig. 3.4. The mainpart takes place on the Multi-Chip-Module (MCM). The signal is synchronized in timing and digitized. After bunch-crossing identification (BCID) and a few other processing steps the signals are serialized for the transmission to JEP and CP. The implementation is realized on a printed-circuit board (PCB) including different submodules on the PPM: the AnIn daughter board, the Multi-Chip-Module, a self-designed Application Specific Integrated Circuit (ASIC) and auxiliary modules.

PreProcessor Module

The PreProcessor Module (PPM) is a 9U VME64xP PCB holding all components for the processing chain of the PPr system. Each module processes 64 channels. The submodules and daughter-boards are mounted on the PPM.

The analog signals are routed directly to the Analog Input daughter-boards (AnIn) through four input connectors. Since one AnIn can handle 16 channels, each PPM is equipped with four AnIns.

From the AnIns the signals are transported to the PreProcessor Multi-Chip-Module (PPrMCM) where the main signal processing takes place. The full processing chain is shown in Fig. 3.4. The digitization of the signals is done using FADC chips while the fine adjustment takes place on one PHOS4 chip [18]. Since the processing is very specified to the experiment a self-designed PreProcessor Application Specific Integrated Circuit (PPrASIC) is used instead of commercial chips. These procedures are BCID and defining the three data streams:

- Two streams represent energy deposits on a $\Delta\eta \times \Delta\phi = 0.1 \times 0.1$ space-grid. These values are transmitted to the Cluster Processor to identify isolated electrons, τ-mesons and photons

- One stream represents energy deposits on a $\Delta\eta \times \Delta\phi = 0.2 \times 0.2$ space-grid. Those data are transmitted to the JEM for the search of jets. In addition, energy sum-values are determined to search for missing E_T and E_T^{sum}

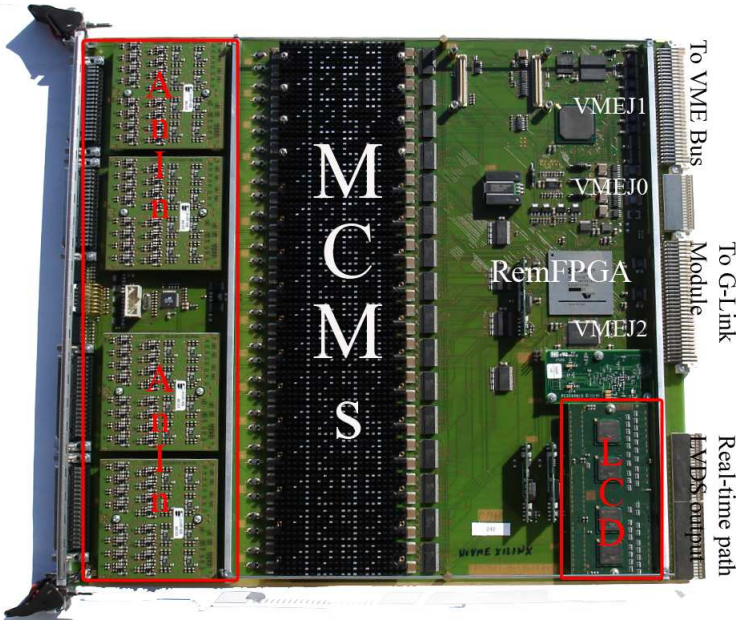

Figure 3.5: Photograph of the PPM

The output of the two separate streams to the CP and the JEM on high speed (480 Mbit/sec) occurs via the LVDS Card Driver (LCD) to backplane connectors and over parallel pair cables to their destination. Careful routing of signals is very important.

The PPM is a "pipelined device" which is driven by the LHC clock. Hence, the systems requires signals from the real-time protocal like the LHC clock, the Level-1 Accept, Bunch-Counter Reset and Level-1 Event-Counter Reset. The TTC system is providing these signals on optical links. A TCM in each crate (for the PPM, as well as for JEM and CPM) receives the signal and distributes them on the backplane. The converting of the TTC protocol for the PreProcessor Module happens on another daughter-board, the so-called TTC Decoder (TTCdec).
Being a standard VME slave module the PPM is interfaced to the VME Bus on the crate backplane. This interface can be used for setting-up ATLAS op-

eration (e.g. hardware-registers, downloading FPGA code, etc.) debugging, control and testing the module in the lab.

The data readout to the DAQ system uses a different path with a higher band-width than the monitoring readout. Both data are separated in the Readout-Merger FPGA (ReM_FPGA). The event-related data are send via a Rear G-Link Transmission Module (RGTM) in serial form to a ReadOut Driver Module (ROD). For monitoring control and later reconstruction, the data are stored using the DAQ system of ATLAS.

Pre-Processor AnIn

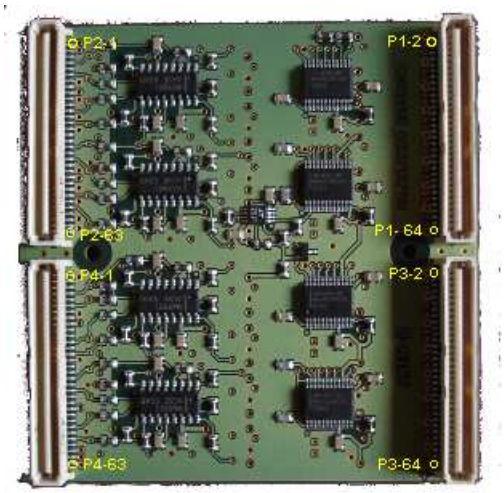

Figure 3.6: Photograph of the AnIn

The Analog Input (AnIn) daughter board receives the incoming differential analog signals from receivers. Four AnIns are mounted on each PPM, each AnIn handles 16 channels arriving through the input connectors.

For each channel two output signals are sent via the PPM to the MCM:

1. a digital signal. The rising edge of the signal represents the point in time, when the analog signal exceeds a voltage threshold. Furthermore it is used for so-called external BCID

2. a uni-polar analog signal. It is used as the input of the digitizing FADC and should have a low impedance

Each AnIn board holds a discriminator to produce the rising edge for each signal. The gain of the uni-polar output is adjustable to match the input-voltage window of the FADC. The "zero-line" offset is also adjustable via a Digital-to-Analog Converter (DAC).

PreProcessor MCM

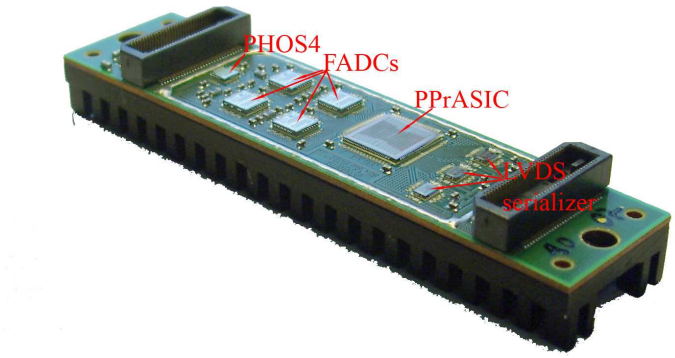

Figure 3.7: Photograph of the PPrMCM

The PreProcessor Multi-Chip-Module (PPrMCM) is the smallest mezzanine card of the PPr system. It is also the central device in the hardware and almost all of the processing takes place on this device. Since one MCM handles 4 channels, 16 MCMs are plugged-on on one PPM. With 124 PPMs a total number of 1984 MCMs is required and together with spare modules 3130 MCMs were produced.

All MCMs are identical in hardware. Nine chips are mounted on every MCM, 4 FADC chips, 1 PHOS4, the PPrASIC and 3 LVDS chips. The chips are facing the PPM motherboard and are covered with brass-lid. Only the 16 heat-conductors are visible.

Each of the 4 Flash Analog-to-Digital Converter (FADC) chips digitizes one channel at a preset phase within each LHC clock-cycle. To synchronize the channels, the 4-channel PHOS4 chip sets the FADC strobe-timing within a LHC clock-cycle of 25 ns with a resolution of 1 ns. The digitized signals are passed to the PPrASIC and, finally to the 3 LVDS serializer-chips sending digital data as a serial stream to the Cluster Processor and the Jet/Energy-sum Processor. Two LVDS channels are associated with the CP, one with the JEP.

PreProcessor ASIC

The PreProcessor ASIC (PPrASIC) plays a key role in the Level-1 PPr system. It was designed in the ASIC-labor of the Kirchhoff-Institut für Physik. The PPrASIC receives digital data from the FADCs. Its task is adjusting the data, stored in the pipeline memory to the same LHC clock cycle, providing dead-time free readout of input data to the trigger, determines the bunch-crossing where the event took place, fine calibration with a Look-Up-Table (LUT) and multiplexing data for efficient use of a fast serial transmission

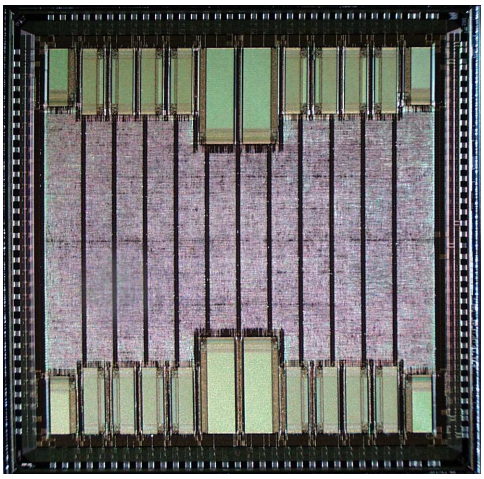

Figure 3.8: Photograph of the PPrASIC

to the CP and JEP. One PPrASIC holds two serial interfaces, each serves 2 channels.

A FADC chip on the MCM digitizes the data. Since the phase of the FADC strobe signal can have a displacement with respect to the LHC clock, resynchronization to the LHC clock needs be done.

The Bunch-Crossing Identification (BCID) allocates the signal to its corresponding bunch-crossing and has to consider two situations:

1. non-saturated pulses, for which pulse shape is constant and independent of amplitude

2. saturated pulses, for which the signal amplitude exceeds the digitization maximum of 250 GeV and is truncated to a fixed value

The algorithm for non-saturated pulses has two logic blocks. First the incoming data is lead to a Finite Impulse Response(FIR)-filter to sharpen the pulse. The second step is to use a peak-finder to get the exact bunch-crossing. Additional a LUT is used for fine calibration of the digitized data after the peak shaping FIR-filter to the deposited E_T.

Saturated pulses are characterized by a series of saturated samples over the period for which the analog signal was above the limit of 250 GeV. Assuming that the peaking-time is unaffected by saturation, the peak position of a pulse of known shape can be determined from the number of saturated samples.

Due to the fact, that cells must be sequenced for the CP data from two neighboring channels on a chip are multiplexed to one single output.

Auxiliary Modules

Apart from the AnIn, MCM and ASIC auxiliary modules are mounted on the PPM, providing further services.

- **LCD** The LVDS Cable Driver (LCD) is responsible for the careful routing and transmission of the serial output streams to the Cluster Processor and the Jet/Energy-sum Processor. The data are sent via parallel pair LVDS cables to the subsequent trigger processors
- **TTCdec** The TTC decoder (TTCdec) daughterboard receives all signals, distributed by the TTC via the backplane. It decodes the data stream and provides individual signals for other daughtboards and modules (mainly the MCM). The TTC signal includes the real-time protocol, e.g. LHC clock, Level-1 Accept, Bunch-Counter Reset and Level-1 Event-Counter Reset
- **CAN bus** To monitor conditions for the operation of electronics, like temperature and power the ATLAS experiment is using the standardized CAN bus system. Standard equipment like powersupplies and fan-units are connected to this system. The PPM is also arranged with a CAN bus to control temperature and electronics

3.3.2 Cluster Processor

The Cluster Processor (CP) processes 6400 electromagnetic and hadronic trigger towers which correspond to 50×64 trigger windows. The architecture of the windows based on trigger towers as shown in Fig. 3.9 (b). Each trigger towers has a size of $\Delta\eta \times \Delta\phi = 0.1 \times 0.1$. The CP is covering the region $|\eta| < 2.5$. 8-bit trigger signals are received from the PreProcessor on about 2000 coaxial LVDS cables. The task of the CP is to provide electron/photon and hadron/tau trigger multiplicity information and RoI information for the Level-2 trigger.

The full system consists of four 9U crates, each crate is equipped with 14 Cluster Processing Modules (CPM). One CPM crate is processing 1/4 of the calorimeter in ϕ over the full pseudorapidity. In this ϕ-quadrant architecture one CPM is processing 4×16 trigger windows. The results from all CPMs are transferred to Common Merger Modules (CMM) in the same crate and these results are transferred to the CTP. The RoI and DAQ data from all CPMs are send to RODs.

3.3.3 Jet/Energy-sum Processor

The Jet/Energy-sum Processor (JEP) performs the jet, missing-E_T and total-E_T algorithms on 0.2×0.2 electromagnetic and hadronic jet elements provided by the PreProcessor. Each of the jet elements consist of 2×2

(a)

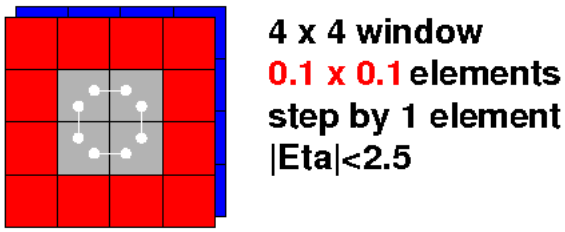

(b)

Figure 3.9: Photograph of the Cluster Processor Module [20] (a) and window size for Cluster Processor (b)

trigger towers, i.e. each element has a size of $\Delta\eta \times \Delta\phi = 0.2 \times 0.2$. The jet algorithms provide options for three cluster sizes as shown in Fig. 3.10 (b): 2×2, 3×3 and 4×4 jet elements.

The JEP system is housed in two 9U crates. One crate is processing two quadrants in ϕ of the jet/energy-sum trigger space. The processing is done on a Jet and Energy-sum Module (JEM) which receives data from the PPr and performs trigger algorithms for a region of 4×8 elements in $\eta - \phi$. To provide the required environment for this region each JEM receives 22 jet elements from its neighbor in $-\eta$ and 11 elements from its neighbor in $+\eta$ and also transmits 22 jet elements to its neighbor in $+\eta$ and 11 to $-\eta$ via the backplane.

Fifteen JEMs in each crate cover a range of $|\eta| < 3.2$, a sixteenth module receives additional FCAL sums which are added to the sum-E_T acceptance region. Each JEM transmits its results of the E_T summation and the jet algorithms to a Common Merger Module in each crate. The data for the CMM contains the E_T, E_x and E_y sums for that JEM and the number of jet clusters passing each threshold.

The JEP also provides data for the DAQ system. Upon a Level-1 Accept input data and RoI, stored in pipelines on each JEM are transmitted to the

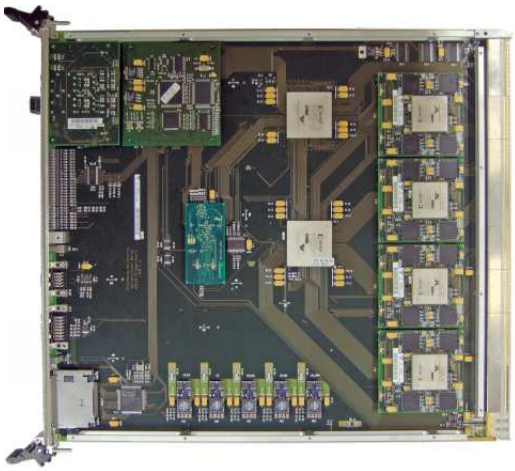

(a)

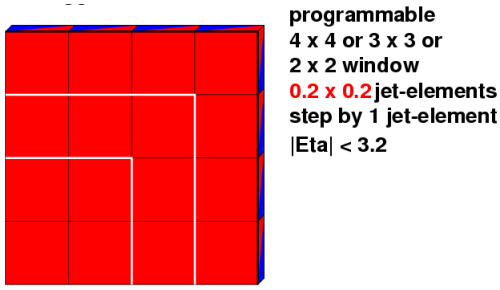

(b)

Figure 3.10: Photograph of the Jet and Energy-sum Module [19] (a) and window size for Jet/Energy-sum Processor (b)

DAQ system and the RoI builder.

Chapter 4

Commissioning and calibration of LVL1

4.1 Strategy of commissioning

The Level-1 Calorimeter Trigger is a complex system build-up of several components with different requests and problems, which must be understood. To guarantee a faultless operation, initial test are conducted checking the correct functioning of all modules and cables. The challenge of commissioning is the huge number of items.

System	Number of crates	Modules/Crate	Total module number
LAr receiver	6	16+2 monitor modules	96+12
Tile receiver	2	16+2 monitor modules	32+4
Receiver summing patch panels			8
PPr	8	16(14)+1 TCM	124+8
CP	4	14+2 CMMs+1 TCM	56+12
JEP	2	16+2 CMMs+1 TCM	32+6
ROD	2	10+1 TCM	20+2
Total	**24**		**412**

Table 4.1: Number of modules in the LVL1 trigger

Tab. 4.1 lists the number of crates and modules. All of them are subjected to operating tests at their individual institutes of production prior to their installation at CERN. Nevertheless commissioning and integration into the complete system makes further tests of crates and modules necessary, e.g. the communication and crosstalk of modules with the crate backplane. Additional cables are installed and tested, checking the connectivity of ev-

ery pin as well as quality checks of signals. An overview of cable numbers and patch panels is shown in Fig. 4.1. Altogether the Level-1 Calorimeter Trigger Group is responsible for 776 analog cables and 1888 LVDS cables. All of these cables need to be checked for correct connections and mapping described in document [21]. The input signal to the PPM as well as output/input signal to further modules like CPM, JEM and ROD have to undergo quality tests.

Another topic of the commissioning is the integration of software, e.g. for monitoring cable tests or different module parameters like temperature and voltage. It is planned to have a fully functional system available in summer 2007.

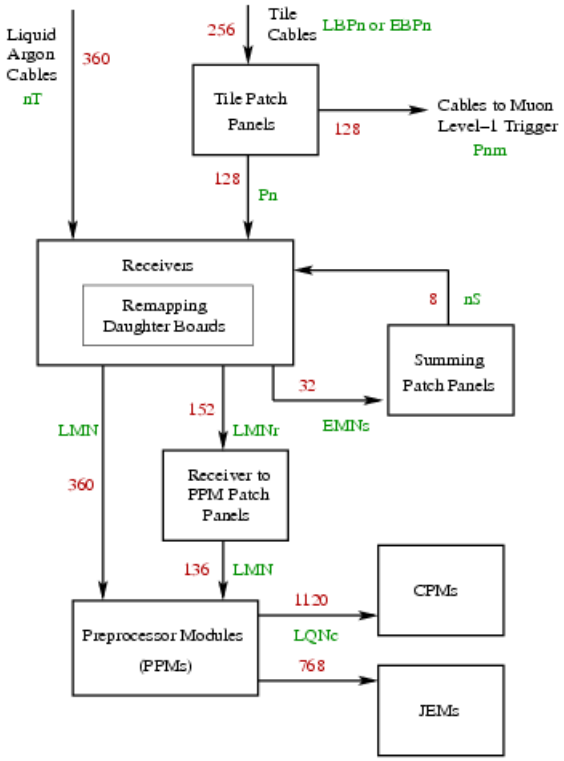

Figure 4.1: Cables and patch panels in the LVL1 trigger system [21]

4.2 Calibration

4.2.1 Goals

Since calibration is essential to ensure a precise operation, a calibration process is not only required when installing and commissioning the system,

but during runs, cosmic runs, at the end of and between LHC fills as well as in longer periods of shutdown. The LVL1 trigger comprises the following parameters, each of them requiring calibration:

- Analog pulse shape and timing have to be compensated by the BCID coefficients and need coarse and fine tuning
- E_T extraction from calorimeters through electronic chain, cables, receivers and FADCs. This needs variable gain amplifiers and a final tuning by look-up tables (LUTs) of the PPMs. Measurements of noise/pedestal level are also essential
- To manage efficiency and rate the calibration of the trigger threshold settings is required. They must be adjustable in steps across eta and phi
- Latency for each readout pipeline memory
- Several timings, e.g. the input timing as the FADC strobe and synchronization delays or internal timings as the clock and the strobe phase for all internal links.

Additional the calibration might possibly discover as yet unknown problems like noise and grounding. These problems needs to be understood and if necessary solved.

4.2.2 Tools

Several tools are used for the calibration. To store and read informations and parameters a database is available as a general tool. It is intended to store everything into the database:

- Calibration and timing settings needed by module services
- All measurements,results and histograms
- Input parameters needed for calibration and timing procedures

As database the POOL Persistency Framework is used. Parameters for each run are coming from configuration files. These files are saved in this database, as well as histograms via GNAM and/or ROOT or ps files. The events are coming from files or monitoring streams. To perform varied calibration runs the database should be usable both online and offline.

The calibration is organized in different runs. Every run serves a special purpose. The next sections describe the individual calibration runs.

FADC DAC Scan

Finding the DAC value needed to set the chosen FADC pedestal value is the object of this scan. Its procedure includes a so-called multi-step run, scanning the DAC value and reading the FADC output. A Histogram FADC output vs. DAC setting is produced and a straight line fitted to determine the slope and offset. The slope, offset and χ^2/ndf should lie in an acceptable range. The DAC settings are needed for all subsequent FADC measurements. A detailed description is given in section 5.2.

Pedestal Run

The pedestal run measures the FADC pedestal noise by collecting events with all electronics on, but no beam or calibration pulses. It creates histograms with pulse height and reject events containing pulses. The mean and sigma of the pedestal is calculated and checked within limits. The pedestal settings are needed for subsequent FADC measurements.

Coarse Timing Scan

Multi-step run and scanning DAQ readout pointers are applied to set the DAQ readout memory offset. To find the pulse maximum, the coarse timing scan searches for five consecutive FADC samples above the pedestal. It checks for single pulse regions with not saturated pulses and a width of exact five samples. As input it needs calibration pulses or beam, FADC DAC and pedestal mean and sigma.

Fine Timing Scan

The fine timing scan measures the PHOS4 settings to sample the analog pulse peak. It also picks the +/- clock edge to capture digital data. This scan may change the coarse timing settings. The procedures of the scan are a multi-step run and scanning the PHOS4 delay. It collects events and finds the peak of the fine timing curve. As the TTC timing and FIFO need to be adjusted for synchronizing input into JEMs/CPMs, this run should be taken with PPM TTC settings already adjusted to achieve system-wide synchronization.

Analog Pulse Shape Measurement

This calibration run measures the analog pulse shape and identifies bad channels. Using events from the fine timing scan the analog pulse shape measurement computes pulse risetime and falltime, peak and the FWHM and compares these parameters to limits. To show the distribution over many channels it fills several histograms.

FIR Filter Coefficients

The next run computes the Finite Impulse Response filter (FIR) coefficients and "drop bits" settings for each trigger tower or groups of trigger towers from the same calorimeter. Using the fine timing pulse shape it set up matched filters. The FIR run does also parabolic fits around five sample points. Calibration pulse data recorded during fine timing are needed for this run.

Electronics E_T Calibration

The Electronics E_T Calibration is the final calibration run. It finds receiver and lookup table values to reproduce the E_T deposits simulated by calibrations pulses. Several procedures are included in this run: setting unity receiver gain, disabling the PPM LookUp Table (LUT), loading FIR filter, executing multi-step run, scanning calo pulse height over a range of non-saturating and labeling events with E_T before main analysis.

The transversal energy is calculated by applying the known E and $\sin(\theta)$. For each point mean and sigma are computed and the PPM response versus injected E_T is fitted. The sigma of data at each energy point and the linear fit χ^2/ndf should lie within predefined limits. To reach the top LUT address with 250 GeV E_T the needed receiver gain is calculated and the LUT parameter is set to give a zero output until FADC pedestal plus 1 GeV threshold is exceeded, and then rise linearly to 250 GeV E_T.

The two calorimeters hold several tools to generate calibration pulses. Whereas the TileCal provides four different tools, the LAr comprises only one option for the calibration of signals. The calibration systems of the tile calorimeter are:

- A movable radioactive source (^{137}Cs γ source) generating light in a scintillator in an identical manner particles from LHC interactions would do
- A laser imitating the calorimeter for each PMT, usable to monitor linearity and gain
- A charge injection system (CIS) which is able to inject charge with a maximum of 800 pC (corresponding to around 800 GeV) in 1 GeV steps. For further details see chapter 5
- A continuous monitoring of minimum bias signals during data-taking

The calibration system of the liquid argon calorimeter is:

- A charge injection system at the front-end electronics. As opposed to the CIS of the TileCal, groups of 16 channels are controlled together

and can only be fired together in a number of fixed patterns, e.g 0-7, 8-15

For the comparison of trigger data with calorimeter data which is described in the next two chapters, common calibration runs are needed. The run will include producing of analog calorimeter signals and summing them to trigger towers within the front-end electronic. The trigger tower signals are send to the Level-1 Calorimeter Trigger, where they are digitized. Both, calorimeter data and trigger data are stored for offline analysis.

Chapter 5

Experimental data

The aim of this study was the development of tools for systematic comparisons of trigger signals with calorimeter signals, its first usage and to develop a fit function for analysis. Quantitative comparisons were done and a first analysis was accomplished.

A Systematic analysis is essential to investigate the influence of the electronic chain and cable on the analog signals. It is expected that the signals alter their behavior regarding pulse height and shape. Since amplitude and signal shape are part of the calibration a good understanding of the effects is essential.

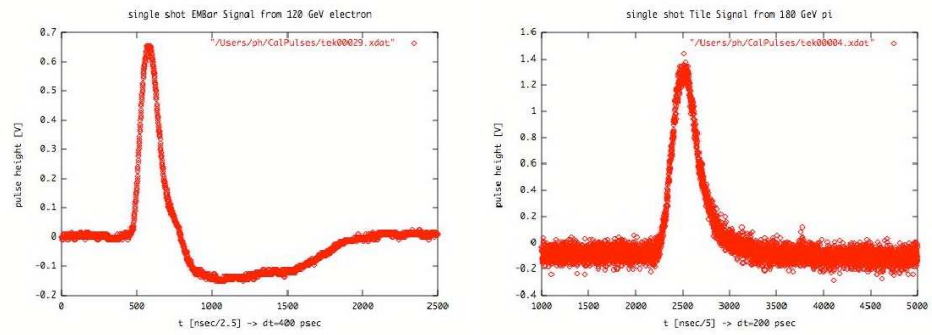

(a) (b)

Figure 5.1: LAr signal (a) and TileCal signal (b), recorded at the testbeam 2004 [24]. Both pulses have a peaking time of $\approx$ 45 ns. The positive part of the LAr signal has a typical length of 3-4 bunch-crossings, the TileCal signal is narrower with 2-3 bunch-crossings

While the calorimeter signals are cosmic data, the trigger signals are produced by a charge injection system. The two data sources used for this study are described in section 5.1. Furthermore data for the trigger and the calorimeter were taken in different sectors of the detector. No systematic

tests were accomplishable but this study shows, how to compare trigger data with calorimeter data and to analyse them. A fit function was developed applicable for trigger- as well as for calorimeter signals.

The analysis was focused on TileCal data, since they were available for recording with the trigger as well as with the calorimeter. The signals from tile calorimeter and liquid argon calorimeter have different pulse forms. The signal of the LAr calorimeter is characterized by a bi-polar form. Only the positive amplitude is useful for the trigger. Unlike the bi-polar pulse of the LAr the TileCal sends a signal with uni-polar pulse form to the trigger. This shape is from converting light to electrons and amplifying the electrical pulse to a detectable signal. The characteristical form of a LAr and a TileCal signal is shown in Fig. 5.1.

5.1 Data sources

As described in chapter 4 several methods are available to generate signals for tests and calibration within the detector and the electronics. These methods are a radioactive source, a laser imitating calorimeter signals, a charge injection system and cosmic muons. Two of these methods were chosen for the comparison of trigger and detector signals.

5.1.1 Cosmic data

During cosmic runs muons originating from cosmic rays are measured in the tile calorimeter. These muons are not coming from the center of the beam pipe, but they are flying from the top down through the detector. In Fig. 5.2 the red lines display the track of a muon. A muon deposits roughly 350 MeV in a single cell. Two trigger modes with different thresholds are utilized for cosmic runs: Back-to-back tower trigger with energy deposition in opposite towers and a single tower trigger where most of the energy is deposited in one tower. The back-to-back tower trigger has a threshold of e.g. 38 mV equal to 1.55 GeV deposited energy, whereas the single tower mode has threshold of about 50 mV corresponding to 2.0 GeV. For the barrel the back-to-back tower trigger and the single tower trigger are applicable. For the extended barrel only the single tower mode is used.

High energetic particles produce light within the scintillator material, which can be measured by photomultiplier tubes (PMTs). The signal is amplified by electronics located next to each PMT (see Fig. 5.4). Each photomultiplier tube provides four outputs:

1. Slow integrator output used for cesium calibration

2. High gain output (0-10 GeV) 1023 counts/800 pC*64 = 82 counts/pC. A muon with 0.2 pC deposition in a cell would produce 17 counts

3. Low gain output (10-1000 GeV) 1023 counts/800 pC = 1.3 counts/pC. The 800 pC full scale is ≈ 700 GeV/channel

4. Analog trigger output derived from the low gain output

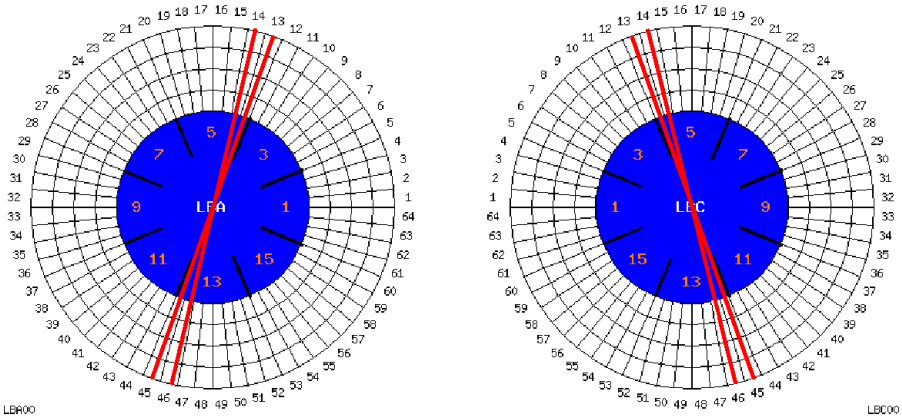

(a) (b)

Figure 5.2: Modules used for the cosmic run 2005 A-side (a) and C-side (b) [26]. Both sides used modules 13, 14 and the opposed modules 45 and 46. The red lines illustrate muon tracks

Since the trigger is designed for high energy objects like electrons and jets it is a challenge to trigger on muons with an average energy deposition of about 2 GeV but a muon is easy to see on the high gain output of the PMT. To increase the output signal the gain of the phototubes can be increased via the high voltage (HV) settings:

$$Gain = \alpha \cdot HV^{\beta}$$

$$HV_2 = e^{\frac{ln(Gain_{increase})}{HV_1} + ln\beta}$$

with $\beta \sim 7$. Examples for a given PMT are:

$$HV(nominal) = 683V \qquad HV(2 * gain) = 754V \qquad HV(3 * gain) = 799V$$

The calorimeter data for this study based on the cosmic run with the run number 1134. It took place in June 2005. As trigger mode the back-to-back tower mode was used and the threshold was set to 38 mV (corresponding to 1.55 GeV) with a triple gain. 3115 events were recorded in a period of almost 64 hours, therefrom 2000 events with an energy > 1 pC deposited charge corresponding to 1 GeV. The setup consists out of 8 modules arranged

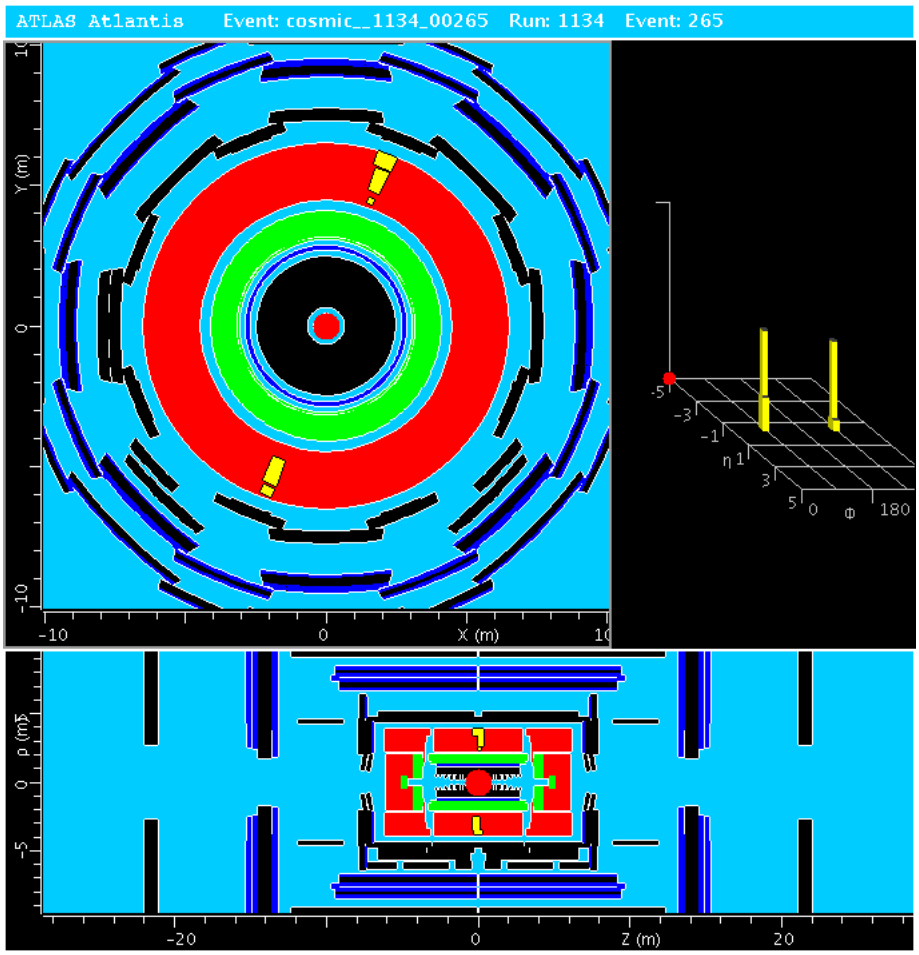

Figure 5.3: Back-to-back tower trigger event displayed with the ATLAS Atlantis Event Display. The muon flew through module A13 and C45, each with tower 1

as 2 top and 2 bottom modules on both A-side and B-side. The upper modules were 13 and 14 as shown in Fig. 5.2 and the corresponding back-to-back modules were 45 and 46. Only the barrel was used with 9 towers in each modules. All together 72 towers were active. Additionally, 8 sets of temporary cables, 8 temporary low-voltage power supplies and 2 cooling units were installed.

The raw data of the cosmic runs were stored on CASTOR, the CERN Advanced STORage manager. To reconstruct ROOT files from the raw data the *Athena* framework is used and additionally every single event can be displayed with *Atlantis* (the ATLAS event display) as shown in Fig. 5.3. Further details of the reconstruction is described in chapter 6.

5.1.2 CIS data

To test the behavior of each read-out channel over its full range and to demonstrate the linearity over the working range, the hadronic calorimeter is equipped with a charge injection system (CIS). It works by discharging a 1% precision capacitor at the input to the pulse shape. Therefore each 3-in-1 card has a pair of 8-bit DACs connected in series to provide a 16-bit dynamic range. The electronic assembling of a photomultiplier tube is shown in Fig. 5.4. The capacitor is located after the divider and is controlled by the 3-in-1 card. This card represents the front-end of the electronic read-out chain and has three functions: pulse shaping and accommodation of the large dynamic range, charge injection calibration and slow integration of the PMT signals for monitoring and calibration.

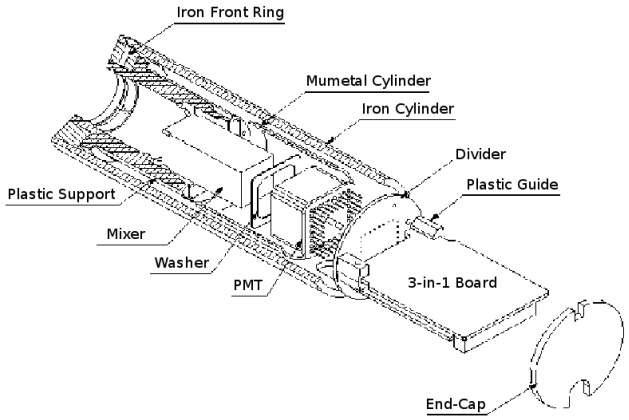

Figure 5.4: PMT block of the TileCal, the CIS is located at the back of the divider [10]

The scintillators in each module are grouped into rectangular cells. These cells are named by the letter of the layer they are located in plus a number. In R-direction the TileCal has four layers: A, B, C and D as shown in Fig. 5.5. Each cell is viewed by a pair of PMTs whereas the cells B and C are viewed by the same pair. The cells of the layers A, B and C have a width of $\Delta\eta = 0.1$ while the D cells, which typically contains less energy have a width $\Delta\eta = 0.2$. Typically five cells are summed to build a trigger tower. This summation is described in chapter 6.

The CIS generates pulses with a different characteristic to physics pulses. The signal of a charge injection is $\sim$10% narrower than a physics pulse, furthermorere the signal from the 3-in-1 contains a "leakage pulse", a small bipolar pulse which has its origin from internal capacitance of the injection switch. As the CIS happens after the PMT it has also a not optimal timing. The path cell→PMT fibres→3-in-1 card→adder cables is optimized so that

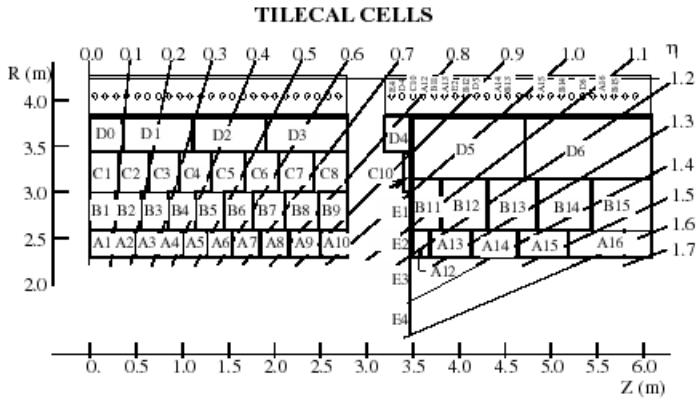

Figure 5.5: TileCal cells in the barrel and the extended barrel sections [30]

the 5 signals building a tower arrive simultaneously at the adder, whereas CIS signals arrive at different time.

The ideal calibration would be a combination of CIS per channel plus corrections and for the timing the Laser/LED system plus fiber corrections which is not described in this document. For more details see [10].

5.2 Pre-Processor data

The Pre-Processor Module provides three different types of data readout. The serial data stream of the real-time path to the Cluster- and Jet/Energy-Processor includes three data streams: two streams contain energy deposits on a 0.1×0.1 grid for the Cluster processor and a third one containing energy deposits on a 0.2×0.2 grid for the Jet/Energy-sum Processor. The signals are sent to the CPMs and JEMs via LVDS cables driven by the so-called LVDS Cable Driver (LCD).

The data readout of event-related data in physics-runs with a high band-width to DAQ and ROD is realized by a Rear G-Link Transmission Module (RGTM). The RGTM sends the serial data on a high-speed optical link to a ROD. During data taking for this study no ROD was available hence data taking via ROD will not be described in more detail.

Since the PPM is a VME64xP slave module, it is interfaced to the VME Bus on the crate backplane. The VME is used to enable tasks like setting hardware-registers, downloading FPGA code or firmware, etc., but it also provides the facility for debugging and/or testing the module. A laboratory crate does not have a full readout facilities, therefore the VME Bus can be used as a low band-width data readout for monitoring. The separation of the RGTM and the VME readout takes place in the ReM_FPGA.

The tools for monitoring VME readout and data taking are described the sections 5.2.1 and 5.2.2.

5.2.1 Online monitoring data

As described above, the trigger data were produced by the charge injection system and monitored with an application of the *ppmMonitoring* package. This package provides *monitoring histograms* which are displayed with the *PMPpresenter* (now called Online Histogram Presenter OHP). The *ppmMonitoring* package is included in the L1 Calo Online Software and contains all three cable test multi-step runs (PPM DAC, PPM FIFO and PPM PHOS4). The appliance of the software and the data taking occur in the electronic cave USA15 on a standard PC next to the LVL1 trigger racks. This allows quick change of the system setup before and during cable tests, e.g. changing cables or checking the right connections. The charge injection system is controlled via PCs located in USA15, too.

The three multi-step runs of the *ppmMonitoring* package are described below:

The PPM DAC scan multi-step run

Since the pedestal and noise contribution vary from channel to channel, the linearity of the FADC counts as a function of the DAC settings needs to be checked for each PPM channel separately. During the run the DAC setting increases stepwise in 1 bit steps. For each step the scan parameter values (DAC settings) and the corresponding raw data (typically a set of 20 FADC samplings) from each PPM channel are read out and stored in a file. The linearity of the system is checked by drawing a profile histogram with DAC values vs. mean of FADC counts for each channel. A *cable test application* determines the DAC settings corresponding to the desired pedestal value (typically 40 FADC counts). The *monitoring histograms* of the analysis of every channel is published on the Online Histogramming server (OH) and displayed with the *PMPpresenter* tool. The DAC scan is necessary to guarantee that each trigger tower is digitized with a zero offset.

The PPM FIFO scan multi-step run

The FIFO scan is executed in order to estimate the pedestal value in each PPM channel using the DAC settings determined by the DAC scan. The raw data (FADC counts) and the scan parameter value (the PHOS4 delay) corresponding to each PPM channel are read out and saved in a file during the run. The file is used to provide 64 1-dimensional histograms of each run and is input to the monitoring package.

The PPM PHOS4 scan multi-step run

The PHOS4 scan determines the optimal PHOS4 delay for each channel. The run scans in steps of 1 ns from 0 to 24 ns through all PHOS4 delays to

find the precise pulse timing of each PPM channel. The results of the run, the PHOS4 settings and the FADC counts are saved in two files which are used to provide an overview of the run: pedestal estimation in each channel, signal amplitude and time characteristics like rise time and FWHM. The PHOS4 scan provides two sets of 64 1-dimensional histograms: one set of histograms to estimate the pedestal in each channel and a second set of profile histograms to reconstruct the pulse shapes and to determine their characteristic (FADC counts vs. time with 1 ns resolution).

To determine the pedestal only the first 500 leading samples (corresponding to 20 bunch-crossings) are used, where no signal resides.

The pedestal histograms as well as the profile histograms of the reconstructed pulse shape can be stored in a ROOT-file for later analysis. One of these files had been used for the comparison of trigger signals with calorimeter signals. An example of a pedestal histogram and a profile histogram is shown in Fig. 5.6.

5.2.2 VME readout data

VME readout was used for the comparison of trigger signals with TileCal signals, since no ROD readout was fully functional. The data taking took place in June 2006 in USA15, using the TileCal charge injections system as signal source. The trigger hardware setup was as follows:

- 8 final tile cables connected through 4 TCPPs via 20 m long cables to two prototype PPMs, one on A-side the other one on C-side.

- The TTC signal (clock plus Level-1 Accept to force readout) was provided by the TileCal TTC system with a trigger rate of about 10 Hz.

- VME readout from the PPMs. The number of raw samples read out in DAC/pedestal runs was as usual 20 but in the PHOS4 scan for the signal reconstruction it was set to 48 raw samples. Since one raw sample corresponds to one bunch-crossing the total length of the signal was 25 ns*48=1200 ns.

Four cables were connected to each PPM. Since modules of the hadronic barrel were used, each consisting of nine trigger towers, 9 of 16 channels per cable were active. The channel routing is shown in Tab. 5.1.

The software used was a composition of online software, scripts, *ppmTest package* and *ppmMonitoring package* and was also prepared for signal tests. The idea was to commission the software which can be used later for systematic signal tests and integrated runs with the calorimeter. A schema of the full setup of the VME run is shown in Fig. 5.7.

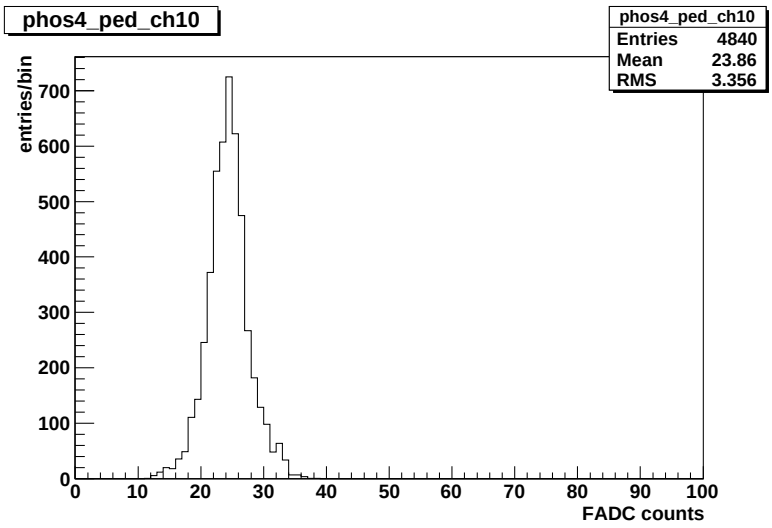

(a)

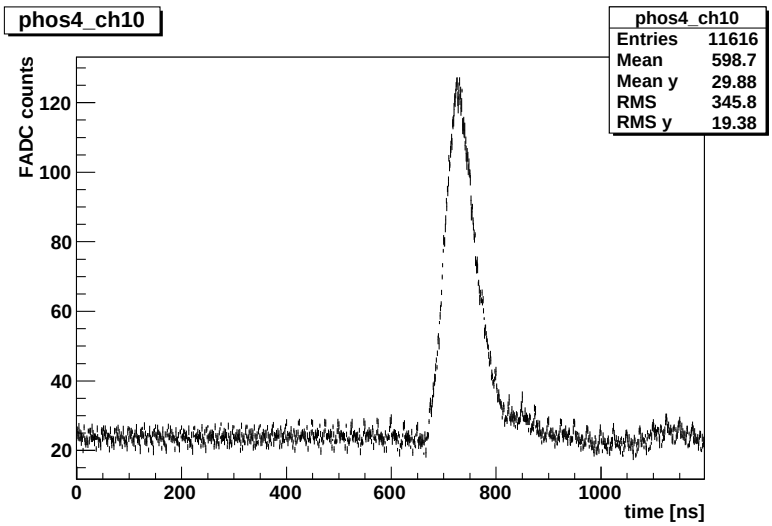

(b)

Figure 5.6: Pedestal histogram (a) and the profile of the reconstructed signal (b). The pedestal histogram is the projection of the y-axis of the profile histogram from 0 ns to 500 ns. The estimated pedestal is 23.86 FADC counts.

The setup of the hadronic calorimeter was sector 13A (in Fig. 5.2 the sectors are illustrated in the blue part in the center of the circle). A sector is assembled with 8 modules. Firstly only 4 modules of sector 13A were active due to problems with the power supplies and the cooling system. Some PMTs had problems and we observed electronic noise in some towers, e.g. up to 10 FADC counts on some towers. Additional two modules in the

second half of the sector had a very high gain, up to a factor 10 higher than other modules. Furthermore both modules were missing tower 9.

TileCal Trigger tower	1	2	3	4	5	6	7	8	9
FADC channel	13	15	14	12	9	11	10	8	5
	29	31	30	28	25	27	26	24	21
	45	47	46	44	41	43	42	40	37
	61	63	62	60	57	59	58	56	53

Table 5.1: Channel routing

The output of the VME readout is a directory which includes different files like two ROOT files including 64 pedestal histograms and 64 profile histograms with the signal reconstruction. An example of each histogram is shown in Fig. 5.6. The upper histogram presents the pedestal of channel 10 (channel numbering starts with 0) where the mean value of the histogram gives the pedestal value for this channel. The lower profile histogram shows the reconstructed signal in channel 10 ranging from 0 to 1200 ns with a resolution of 1 ns. 11616 entries implies an average of 9.68 entries/bin. The high number of entries originates by the fact that the trigger is read out with a rate of 10 Hz provided by the TTC system of the TileCal. This means that the signal shown in the profile histogram is not a single pulse but an overlapping of many pulses with the same timing and amplitude. Due to inconsistent of the pedestal the profile shows a sawtooth structure.

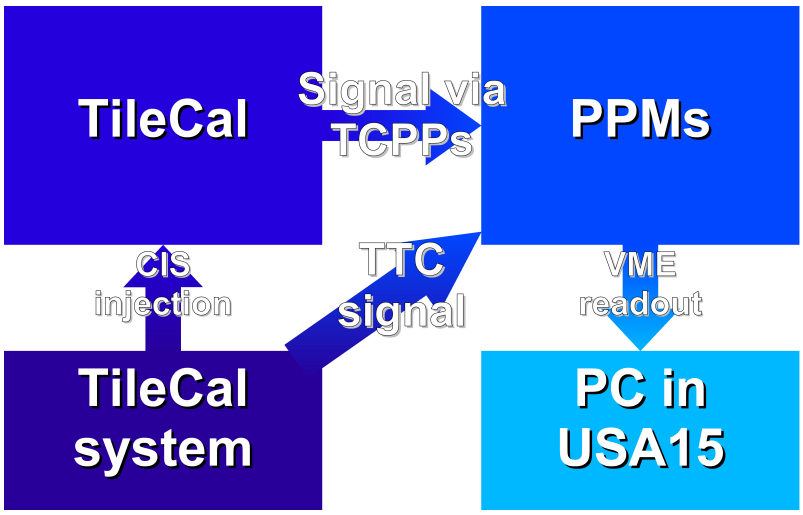

Figure 5.7: Schema of the VME readout setup. The TileCal system provides the TTC signal and controls the charge injection system. The readout of the PPM took place in USA15 on standard PCs.

The *ppmTest package* provides a subdirectory including ROOT files for each PPM. The data in these files contain the average value for each bin, i.e. each histogram is representing an average pulse with 1200 entries.

Chapter 6

Analysis and Comparison

The topic of this study is the comparison and analysis of trigger signals with calorimeter signals. Two types of data source are available: data from cosmic muons for the tile calorimeter and CIS signals for trigger data. The comparison and analysis is made in three steps:

- Data from cosmic runs are stored as raw data on CASTOR. Using the *Athena* framework they need to be reconstructed. A detailed description of reconstructing data with *Athena* is given in section 6.1
- Data from TileCal were taken with 9 samples corresponding to 9 bunch-crossings (maximum are 15 samples) and a resolution of 25 ns, whereas the PPM data were taken via VME readout with a resolution of 1 ns and a width of 48 samples. A software was developed, converting the data to the correct mode and comparing trigger output with calorimeter output
- To analyse the signals a fit function was developed to fit both, signals coming from the trigger and signals coming from the calorimeter

6.1 Offline signal reconstruction

6.1.1 Athena concepts

Athena is a controlled framework implemented in an underlying architecture called *Gaudi*. The *Gaudi* project is a development of the LHCb collaboration, which was adopted by ATLAS. Several concepts specific to the ATLAS software environment are contained in *Athena*.

The *Athena* framework is an application in which developers plug in their code and that provides most of the common functionality and communications between different components. Examples for components are algorithms, services and job option files or Python scripts.

The *Athena* application accepts input data, processes it and generates new output data. The processing of the data includes several algorithms, e.g. track finding and fitting, the association of calorimeter hits into cluster and towers, and the association of particle types with tracks and cluster. The services provide different abilities like histograms.

A job options file controls the configuration of an *Athena* application at run time. Written as a conventional text file (by default called `jobOptions.txt`) it is editable for specifying algorithms or implementing services. Using Python scripts for the job options file has the advantage that it can be used both for configuration and for interactive sessions, since Python is a interpreted, interactive object-oriented programming language.

6.1.2 Reconstruction of TileCal cosmic run data

The ATLAS software environment is based upon the concept of hierarchical packages, depending on each other. A typical package is a set of C++ classes, grouped together with their interfaces and implementation files. Kept in a centralized code repository the packages are managed by the Concurrent Versions System (CVS). To accomplish a reconstruction first an environment needs to be build. Using the Configuration Management Tool (CMT) all packages corresponding to run type (cosmic run, CIS, etc.), system (TileCal, LAr, etc.), *Athena* release, etc. needs to be extracted and compiled.

To reconstruct TileCal data of cosmic run 1134 release *Athena 11.0.2* was used. The raw data of each cosmic run are stored on CASTOR, where they are available for offline procedures. Additional to the standard options several special options can be controlled by setting them to True or False within the job options file *jobOptions_TileMobiCosmic.py*. These options are:

- **doTileNtuple** creates a ntuple with all channels contained in the raw data and writes it in a ROOT file
- **doCaloNtuple** creates a ntuple with the calorimeter cells contained in the raw data and writes it in a ROOT file
- **doCreatePool** creates a ESD POOL file with Tile cells for data management
- **doAtlantis** creates XML files for *Atlantis*, an event display tool for ATLAS

For the reconstruction of signals the two ntuple options were set to true, additionally the option producing XML files was activated to display the event. The ROOT file includes one or more so-called trees, depending on the settings of the job options file. The ROOT file created for cosmic run 1134 is *tiletb_1134_1.root*. Its structure is shown in Fig. 6.1. Each tree has

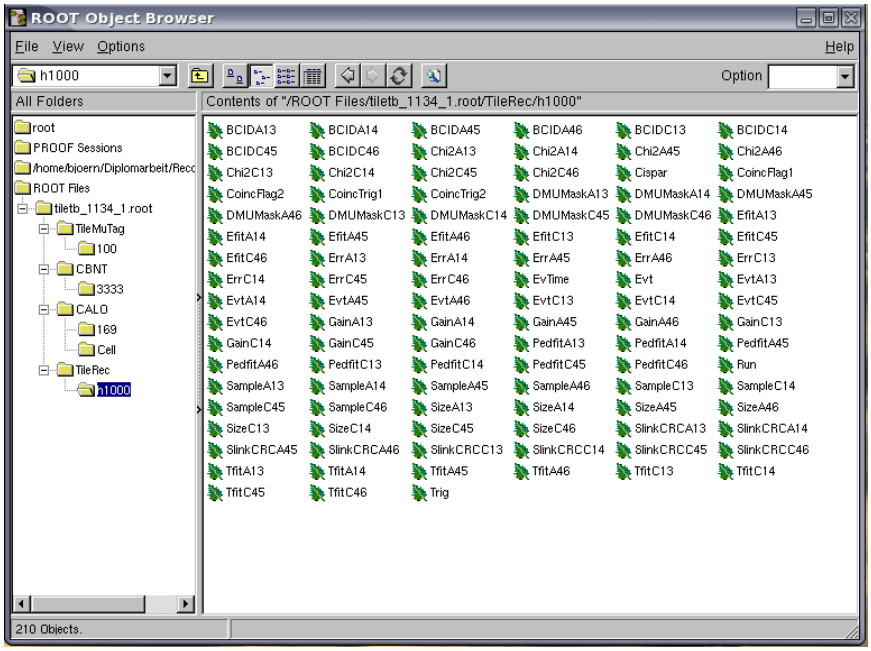

Figure 6.1: Structure of ROOT file, created with *Athena*

a substructure, so-called leaves. The following ntuple variables (leaves) in TileRec/h1000 contain all information needed to reconstruct a signal:

- **Sample...** ADC samples (9 samples per channel, 48 channels)
- **Efit...** Energy per channel calculated by the least-squares fit method
- **Tfit...** Signal timing per channel in ns by the least-squares fit method
- **PedFit...** Pedestal per channel calculated by the least-squares fit method

All variables are named like SampleA13, SampleA14, etc. meaning the ADC samples for module A13 and A14 respectively. Eight modules in the barrel were active during cosmic run 1134: 13, 14, 45 and 46 both on A- and C-side. Each variable contains cell information. A single cell is read out by a pair of PMTs. Since the LVL1 trigger uses signals from trigger towers, one component of the offline software is building trigger towers with this cell information.

6.2 Signal fitting

A typical signal, generated within the front-end electronics of the tile calori meter and recorded via VME readout of the PPM is shown in Fig. 6.2 (a).

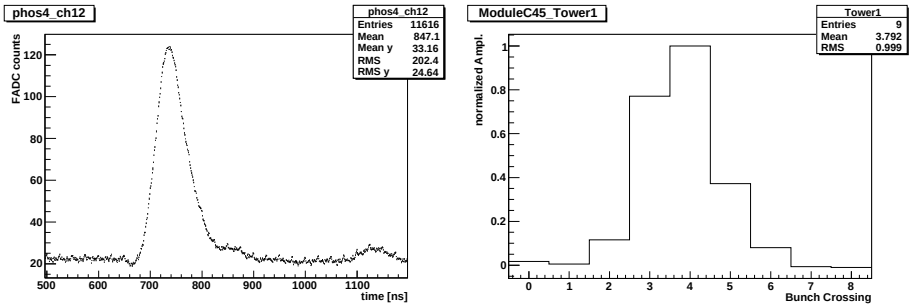

(a) (b)

Figure 6.2: PHOS4 profile of a CIS pulse between 500 ns and 1000 ns (a) and TileCal signal recorded at cosmic run 2005 (b)

The pulse is characterized by a short rise time (10%-90% of peak maximum) and a wide tail. Each signal coming from the detector looks similar but differs in several parameters to each other: amplitude height, rise time, peak position and FWHM.

The pulse shown in Fig. 6.2 displays the analog input to the PPM. With a resolution of 1 ns it does not represent a typical digital readout. By default a signal stored with the DAQ system of ATLAS contains 5 digital samples, each sample is one bunch-crossing (25 ns) wide. A 9 sample signal from TileCal is shown in Fig. 6.2 (b).

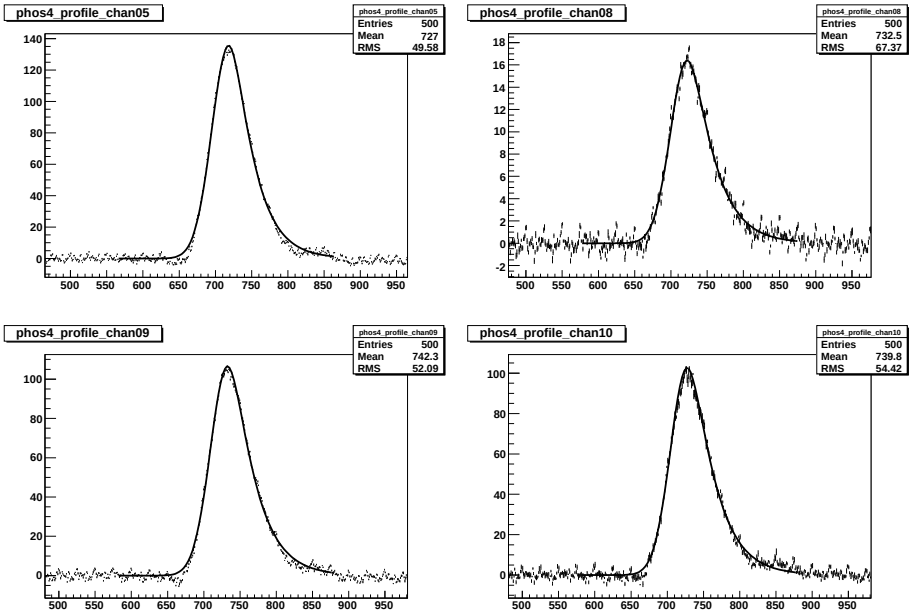

Figure 6.3: Fitted PHOS4 profiles with 1 ns resolution, channel 5 and 8-10

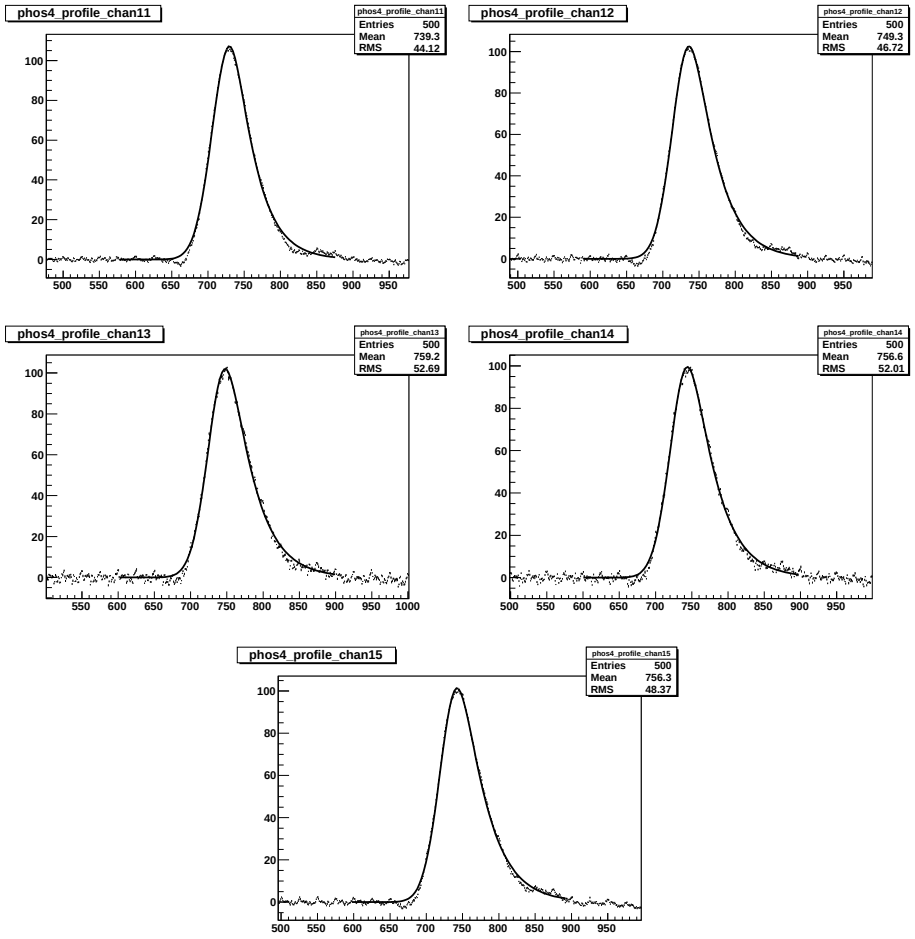

Figure 6.4: Fitted PHOS4 profiles with 1 ns resolution, channel 11-15

To visualize the characteristic pulse shape, a fit functions is applied to the digital samples of a signal. It was found to give the best description by using different functions, one for the rising-, a second one for the trailing edge. The left peak side can be described with a gaussian distribution whereas a landau distribution is used for the right side. Actually a landau distribution describes the energy loss of moving ions in matter. The fit function is defined as:

$$f_1(x) = A \cdot e^{-\frac{1}{2}\frac{(x-x_{max})^2}{\sigma_1^2}-\frac{1}{2}} \qquad for\ x < x_{max}$$

$$f_2(x) = A \cdot e^{-\frac{1}{2}(\frac{x-x_{max}}{\sigma_2}+e^{-\frac{x-x_{max}}{\sigma_2}})} \qquad for\ x > x_{max}$$

with the amplitude A, σ_1 and σ_2 for the standard deviation of gaussian distribution and the landau distribution respectively and x_{max} as the peak position. The two different functions are linked by the same amplitude

and peak position. Overall four parameters describe the characteristics of the signal. The PHOS4 profiles of channels 5 and 8-15 fitted with this fit function are shown in Fig. 6.3 and Fig. 6.4. Future analysis will based on the comparison of width of the rising edge σ_1 and of the trailing edge σ_2. The height of the amplitude will be a feature of the calibration.

6.3 Data comparison

6.3.1 The *CombineTileCalPPM* package

The next step of the study was the development of a software comparing trigger signals with calorimeter signals. It is used to do offline analysis and quality checks of trigger signals. The *CombineTileCalPPM* package is based on C++ class and includes four programs:

- **main.cxx** is the starting program
- **Tile.cxx** processes calorimeter signals from the TileCal
- **Ppm.cxx** processes trigger signals coming from the PPM
- **CombineTileCalPPM.cxx** combines the two signal types

A schematic overview of the package is shown in Fig. 6.5. Executing the program *main.cxx* starts the software. First of all two inputs are expected. The first one is the number of the module, where a cosmic run event took place. One single module or a combination of opposite modules is selectable. The second input is the event number. Since a run includes up to several thousand events, one event needs to be specified. When running *main.cxx* all classes are called successively.

Tile.cxx

The program *Tile.cxx* processes TileCal signals reconstructed as described in section 6.1. The event number input as well as the module number input are passed to this class. Handling the data contains several steps:

- Reading the ROOT file (*tiletb_1134_1.root*)
- Determining the pedestal to subtract it from the signal
- Building trigger towers, subtracting the pedestal and shifting the peak
- Normalizing the amplitude to 1 and fitting the signal
- Creating and providing all histograms to *CombinedTileCaloPpm.cxx*

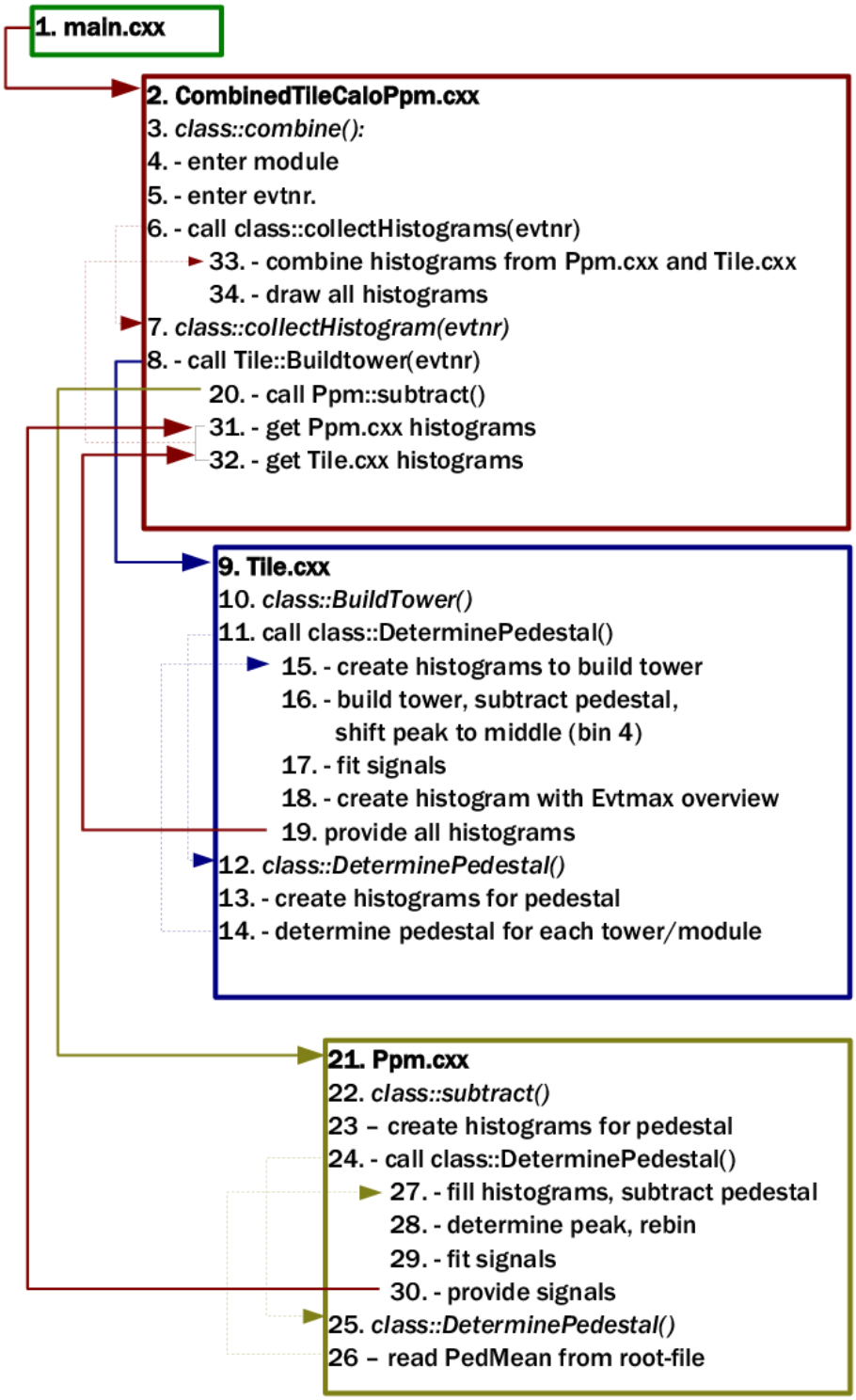

Figure 6.5: *CombineTileCalPPM* package overview

Since the reconstructed data include cell information the script needs to build trigger towers to compare them with trigger signals. The construction happens by summing all cells building a trigger tower. The numbers are listed in Tab. 6.1. Each cell is read out by a pair of photomultipliers, each PMT represents one channel. The geometry can be seen in Fig. 6.6.

η	**Trigger Tower**	**PMTs by cell**	**PMTs by position**
0.0-0.1	T1	A1R A1L BC1R BC1L D0R	5 2 3 4 1
0.1-0.2	T2	A2R A2L BC2R BC2L D1L	9 6 7 8 14
0.2-0.3	T3	A3R A3L BC3R BC3L D1R	11 10 13 12 15
0.3-0.4	T4	A4R A4L BC4R BC4L D2L	19 16 17 18 26
0.4-0.5	T5	A5R A5L BC5R BC5L D2R	21 20 23 22 27
0.5-0.6	T6	A6R A6L BC6R BC6L D3L	25 24 29 30 40
0.6-0.7	T7	A7R A7L BC7R BC7L D3R	31 28 35 36 43
0.7-0.8	T8	A8R A8L BC8R BC8L	37 34 41 42
0.8-1.0	T9	A9R A9L B9R B9L A10R A10L	39 38 45 46 47 48

Table 6.1: Trigger tower building: the first character gives the layer (A-D), the number gives the cell and the second character stands for the L(eft) or R(ight) PMT

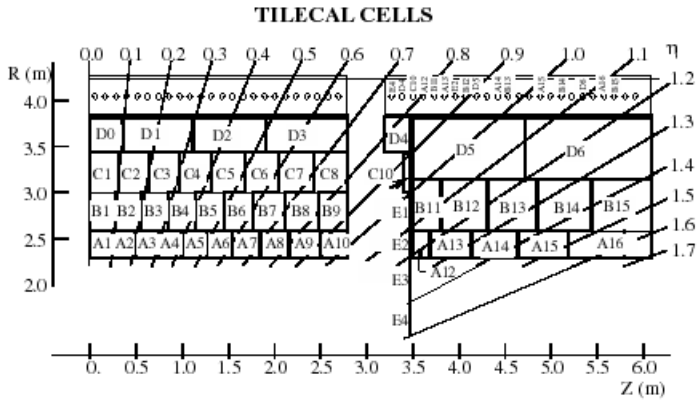

Figure 6.6: TileCal cells and trigger towers in the barrel and the extended barrel sections [30]

The next step is subtracting the corresponding pedestal from each tower and shifting the peak. To compare two pulses their peaks are overlapped. The overlapping needs the peak being located at the same position. After BCID and synchronization on the PPM the middle sample would contain the peak (e.g. 3 of 5, 5 of 9,etc.). Since the cosmic run 1134 has 9 samples it was chosen to have the peak on sample 5. Where this is not the case it

needs to be shifted.
The final step is normalizing the amplitude to 1, fitting the signal, creating histograms and make them available to *CombinedTileCaloPpm.cxx*.

Ppm.cxx

The class *Ppm.cxx* evaluates trigger data from the PPM and converts VME readout into the right format. Procedures of this class are:

- Reading the ROOT file (created by PHOS4 scan, see 5.2)
- Determining the pedestal to subtract it from the signal
- Creating histograms and subtract the pedestal
- "Rebinning" histograms
- Normalizing the amplitude to 1 and fitting the signal
- Providing all histograms to *CombinedTileCaloPpm.cxx*

Whereas the VME output of the PHOS4 scan represents the analog input signal with 1 ns resolution, calorimeter data and the typical digital readout via the DAQ system consists of samples, each sample corresponding to one bunch-crossing (25 ns resolution). Opposed to the calorimeter pulse with 9 samples (225 ns length) pulses from the PHOS4 scan have a length of 48 samples (1200 ns). To "rebin" a 1 ns resolution histogram a cut-off 112.5 ns left and 112.5 ns right of the determined peak is done. The cut-off creates a new histogram with a centralized peak and a width of 225 ns. For simulating the digitization with 9 samples, 9 areas are defined, each including 25 analog bins. Bin 13 of each area gives the "digital" value of a sample. As an alternative the average of all 25 bins can be calculated.

The final steps are normalizing the amplitude to 1, fitting the signals and providing the histograms.

CombinedTileCaloPpm.cxx

The script *CombinedTileCaloPpm.cxx* calls the two classes *Tile.cxx* and *Ppm.cxx*. Having received their histograms it combines the trigger tower built by *Tile.cxx* with the corresponding tower of *Ppm.cxx*. The resulting histograms are stored in a ROOT file. This file contains several sub-directories and has the following structure: *filename*.root/Evtnr.../*module-number*. Each module sub-directory contains a composition of histograms. An example of histograms is shown in Fig. 6.7. Both histograms show the same cosmic event but in opposite towers. Fig. 6.7 (a) displays the event in tower 1 of module A13. The opposed tower, tower 1 of module C45, is shown in Fig. 6.7 (b). In Fig. 5.3 the same event is displayed with the

Atlantis event display. Channel 13 from the PPM VME readout is used as comparative trigger data. This channel corresponds to tower 1 as shown in Tab. 5.1.

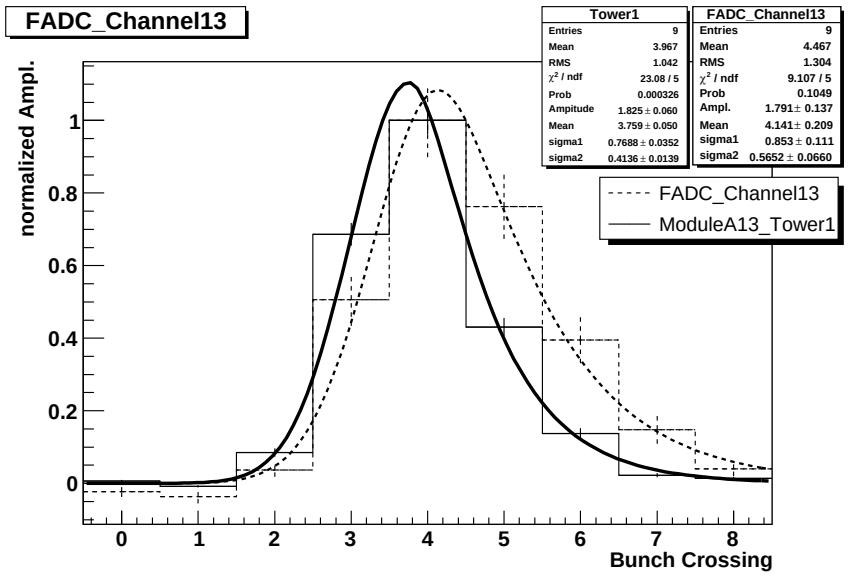

(a)

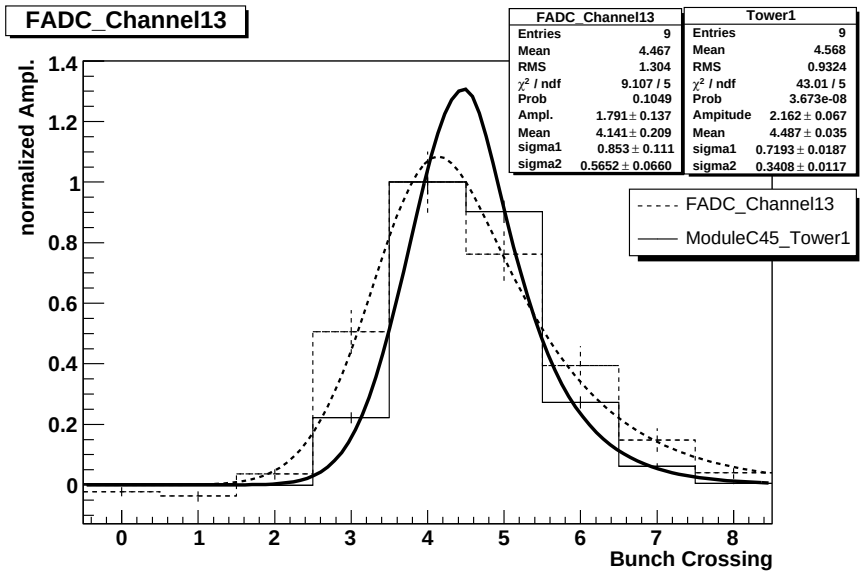

(b)

Figure 6.7: Combination of PPM signal channel 13 (dotted line, corresponding to Tower 1) with cosmic run event no. 265, module A13 (a) and C45 (b), each with tower 1. The Atlantis event display of the cosmic run event is shown in Fig. 5.3

6.3.2 Results and Interpretation

The use of differential origin excludes a systematic analysis. Nevertheless, the results of the combination permits some interpretations. As shown in Fig. 6.7 the combined signals are not situated on top of each other. The unknown timing of signals from cosmic runs is the main contribution to this adjustment. Furthermore samples from cosmic run readouts do not contain necessarily the amplitude. Due to heavy trigger conditions it is difficult to trigger on the peak of a cosmic muon signal. In Fig. 6.7 (a) the peak of the calorimeter signal is located on the right hand of the fifth sample, in Fig. 6.7 (b) it is located on the left hand. During a combined run of trigger and calorimeter, signals will be read out with the same Level-1 Accept. This guarantees the adjustment of the signals for an easy comparison.

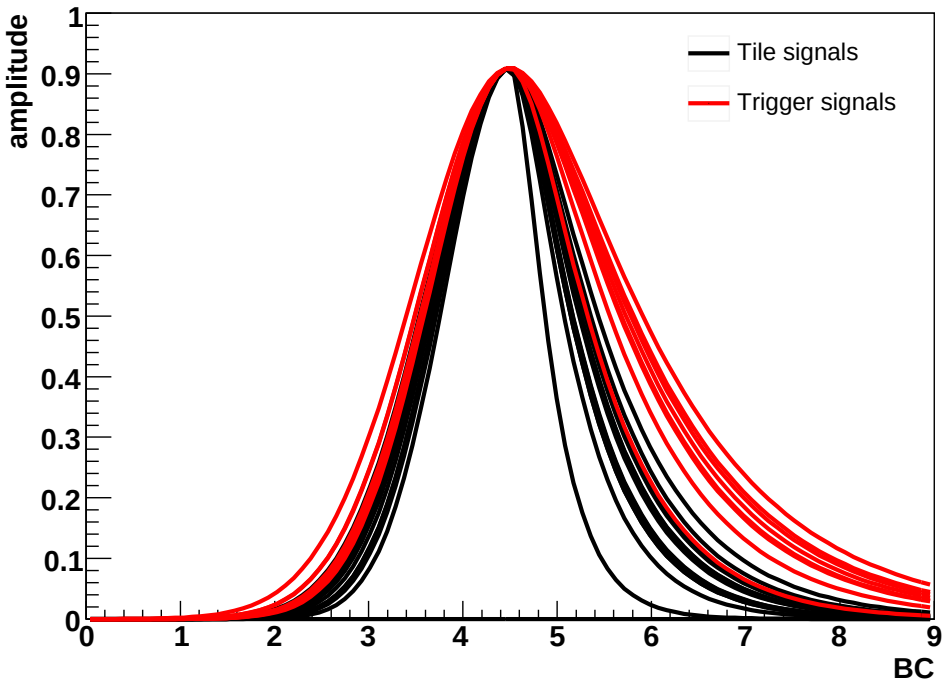

Figure 6.8: 16 TileCal (black) and 9 trigger (red) signals. The calorimeter signals are located in module A13, tower 1 and were recorded at the cosmic run. The trigger signals are coming from 9 towers in the same module recorded via VME readout

The normalization of the amplitude to 1 assumes the peak located on sample 5. Since this is not the case the amplitude of the fitted signals is higher than the digital signal. For calorimeter pulses the effects is shown clearly. The peaks of both TileCal pulses are shifted with reference to sam-

ple 5 (starting with 0 it is Bunch Crossing 4). To avoid a demanding fit amplitude the normalization should occur after fitting the signal.

To get an impression on the disagreement of trigger and TileCal signals the fit of 16 calorimeter and 9 trigger pulses are drawn in the same histogram (Fig. 6.8), all peaks located at the same position and normalized. As expected signals digitized on the front-end electronics of the detector (black) are narrow than signals from the PPM (red). This effect could be caused by the impact of the electronics and cables on the analog signals. Systematic tests with identical signals are needed to prove this effect. Tables 6.2 and 6.3 shows the standard deviation σ_1 and σ_2 for the calorimeter signals and PPM signals respectively. The width of the rising edge σ_1 is about 15% wider for trigger than for calorimeter signals, the width of the falling edge is even about 30% wider.

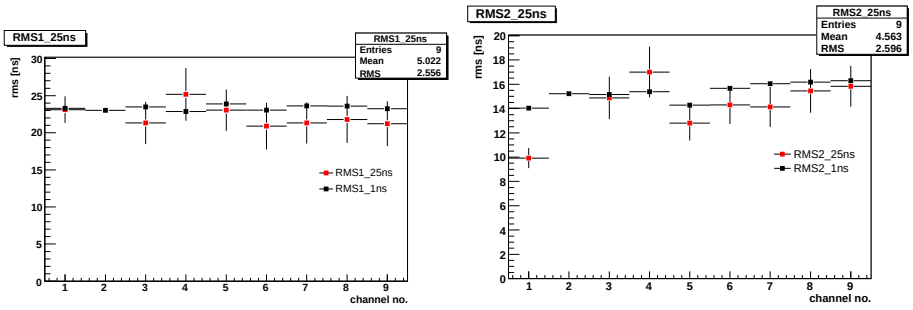

(a) (b)

Figure 6.9: σ_1 (a) and σ_2 (b) for the 9 active channels in a TCPP→PPM cable each with the PHOS4 scan (red) and the rebinned histogram (black)

To verify whether the rebinning of the trigger signals was done accurately the fit parameters of the PHOS4 scan histogram with 1 ns resolution is compared with the fit parameters of the rebinned histogram. The PHOS4 scan displays the analog signal as input to the PPM. Hence the fit of the PHOS4 profile gives an exact description of the pulse. Comparing the PHOS4 scan fit with the fit of the rebinned histograms will check the accuracy of the rebinning. The parameters σ_1 and σ_2 for both formats are shown in Fig. 6.9 (a) and (b) respectively. The standard deviation of the PHOS4 scans are drawn red and black for the rebinned histograms. Except channel 2 all channels have nearly the same parameter values both for 1 ns and 25 ns resolution. The failure in channel 2, which can be also seen in Tab. 6.3 can be explained by some problems with this channel. As shown in Fig. 6.3 and Fig. 6.4 it had lower energy with about 18 FADC counts instead of 100 FADC counts and bad statistics. Due to the agreement of both σ's a good functionality of the fit function can be assumed.

The difference between signals produced by physics particles and signals

produced by the charge injection system is also not included in the comparison. For tests and quality checks the same signal source will be used for both calorimeter data and trigger data. In that case it is irrelevant whether the pulse is generated via charge injection or by particles from cosmic runs, beam gas collisions or other sources.

Event Number	σ_1 [BC]	σ_2 [BC]
76	0.8784 ± 0.027	0.2772 ± 0.0155
131	0.8299 ± 0.032	0.387 ± 0.018
205	0.8591 ± 0.04	0.3233 ± 0.013
244	0.7204 ± 0.0446	0.3578 ± 0.0132
265	0.7688 ± 0.0352	0.4136 ± 0.0139
305	0.8454 ± 0.0443	0.3543 ± 0.0244
419	0.8354 ± 0.0835	0.3632 ± 0.0177
441	0.8092 ± 0.0308	0.3153 ± 0.0161
461	0.8076 ± 0.0331	0.3216 ± 0.0177
495	0.681 ± 0.037	0.4517 ± 0.0157
750	0.8517 ± 0.0279	0.3122 ± 0.0157
856	0.7358 ± 0.0523	0.3834 ± 0.0227
913	0.7374 ± 0.0546	0.3122 ± 0.0202
916	0.794 ± 0.043	0.1788 ± 0.0194
953	0.8683 ± 0.0509	0.3645 ± 0.0258
974	0.7972 ± 0.046	0.3914 ± 0.0223

Table 6.2: Standard deviation σ_1 and σ_2 of several cosmic muon events, each in tower 1 of module A13. BC $\equiv$ 25 ns

Trigger Tower	σ_1 [BC]	σ_2 [BC]
1	0.9246 ± 0.9246	0.397 ± 0.033
2	-0.6567 ± 0.3047	-1.807 ± 0.501
3	0.8526 ± 0.1135	0.595 ± 0.07
4	1.007 ± 0.142	0.6803 ± 0.0836
5	0.9219 ± 0.1116	0.5119 ± 0.0572
6	0.8355 ± 0.1257	0.5717 ± 0.0625
7	0.853 ± 0.111	0.5652 ± 0.066
8	0.8718 ± 0.127	0.618 ± 0.072
9	0.8488 ± 0.1208	0.6332 ± 0.0671

Table 6.3: Standard deviation σ_1 and σ_2 for trigger signals

A systematic test and analysis would look on the behavior of signal width and amplitude at different energies, e.g. linearity. For each channel

the "changing factor" from calorimeter to trigger signal will be calculated and if there is a big range among of this factor, i.e. the histograms are identical in their proportions.

Chapter 7

Summary and Outlook

This thesis describes the development and application of a test-software for quality checks of trigger signals. The PreProcessor system of the ATLAS Level-1 Calorimeter Trigger receives analog signals from the electromagnetic and hadronic calorimeter. Its task is the digitization of the analog input signals, bunch-crossing identification, transverse energy determination and transmission of serial output streams to subsequent trigger processors. The test includes the comparison of analog trigger signals with calorimeter signals which are digitized in the front-end electronics close to the detector.

Two different types of signals were available: cosmic run data as tile calorimeter signals, and for trigger data pulses were generated by the charge injection system of the TileCal. The digital format of the calorimeter data contains 9 samples. Since they are stored as raw data the calorimeter signals needed to be reconstructed by using the framework *Athena*. The readout of the PreProcessor Module displays the analog input of the Level-1 Trigger. To compare them with digital TileCal data a subsequent digitization had to be accomplished. To analyse the pulses a fit function as a combination of of gaussian and landau distribution was developed.

The aim of quality tests is analysing the influence of electronics chain, like 70 m long cables, modules, etc. on the analog trigger signals. The standard deviation of the rising and falling edge is an indicator on the width of the signal, whereas the height of the amplitude can be used for the energy calibration.

The test-software, presented in this thesis gives the environment for systematic quality checks of trigger signals. Initial tests and first analysis showed the expected effects to the trigger signals quantitative. The rising edge of analog pulse recorded with the PPM is about 15% wider than digital calorimeter signals, whereas the falling edge is about 30% wider. Future tests will use the same signal source (CIS, laser, ^{137}Cs, etc.) for trigger and TileCal or LAr data. Furthermore trigger and calorimeter will use the standard readout stream of the ATLAS experiment. The quality tests and

analysis are components of the commissioning and calibration of the Level-1 Trigger.

Currently the first full PPr crate with 16 PPMs is installed at CERN. The commissioning for the complete Level-1 Calorimeter Trigger is scheduled for summer 2007.

Bibliography

[1] Donald H. Perkins: Introduction to High Energy Physics, 4th edition

[2] J. Pumplin, D.R. Stump, J. Huston, H.L. Lai, P. Nadolsky and W.K. Tung: New Generation of Parton Distribution with Uncertainties from Global QCD Analysis, MSU-HEP-011101, 2006

[3] N. Cabibbo: Phys. Rev. Lett. 10, 531-533 (1963)

[4] M. Kobayashi, H.Kondo and T. Maskawa: Prog. Theor. Phys. 49, 643 (1973)

[5] E. J. Eichten, K. D. Lane and M. E. Peskin: Phys. Rev. Lett. 50, 811 (1983)

[6] ATLAS Level-1 Trigger Technical Design Report, ATLAS TDR-12, 1998

[7] ATLAS Trigger Performance, CERN/LHCC 98-15, 1998

[8] LHC Design Report, cernrep/2004-003-v1, 2004

[9] ATLAS Detector and Physics Performance Technical Design Report, ATLAS TDR 14, 1999

[10] ATLAS Tile Calorimeter Technical Design Report, CERN/LHCC 96-42, 1996

[11] Calorimeter Performance Technical Design Report, CERN/LHCC 96-40, 1997

[12] Muon Spectrometer Technical Design Report, CERN/LHCC 97-22, 1997

[13] ATLAS High-Level Trigger, Data Acquisition and Controls, ATLAS TDR-016, 2003

[14] CERN Document Server, http://cdsweb.cern.ch/

[15] Paul Hanke: The Pre-Processor Module (PPM) for the ATLAS Level-1 Calorimeter Trigger, 2005

[16] Paul Hanke: The Pre-Processor "Multi Chip Module" (PPrMCM) assembly in the ATLAS Level-1 Calorimeter Trigger Pre-Processor system, 2005

[17] R.Achenbach, D. Husmann, M. Keller, K. Mahboubi, C. Schumacher: Pre-Processor Asic Design Guide, 2002

[18] CERN-MICROELECTRONICS GROUP: PHOS4 - 4 Channel delay generation ASIC with 1 ns resolution, Datasheet/Rev 1.2

[19] Eric Eisenhandler: Level-1 Calorimeter Trigger Status, ATLAS Overview Week Stockholm, July 2006

[20] Richard Staley: CPM Status (+RPPPs, CAM), Level-1 Calorimeter Trigger Joint Meeting, November 2006

[21] L1Calo Group: Level-1 Calorimeter Trigger: Cable Mappings and Crate Layouts from Analogue Inputs to Processors, ATL-DA-ES-0036, October 2006

[22] Alan Watson, C.N.P. Gee: Level-1 Calorimeter Trigger Calibration, Tatra Mountains 2004

[23] C.N.P. Gee: Calibration Overview, Level-1 Calorimeter Trigger Joint Meeting, November 2006

[24] Paul Hanke: The Pre-Processor System in the ATLAS Level-1 Calorimter Trigger, November 2005

[25] Athena Core software, http://atlas-computing.web.cern.ch/atlas-computing/packages/athenaCore/athenaCore.php

[26] TileBarrelCommissioning, https://twiki.cern.ch/twiki/bin/view/Atlas/TileBarrelCommissioning

[27] Jose Maneira: Cosmic ray analysis with Tile Calorimeter, ATLAS Calorimetry Performance Plenary, CERN July 2005

[28] G.Schlager: Outcome of the Tile cosmic run in the pit, CERN calorimetry group meeting, July 2005

[29] Kelby Anderson: Tile plans for commissioning and cosmic ray, Second North America ATLAS Physics Workshop 2005

[30] TileCal Trigger Towers, http://atlas.web.cern.ch/Atlas/SUB_DETECTORS/TILE/elec/adder/geometry.html

[31] Frederik Rühr: Initial Tests of the ATLAS Level-1 Trigger Pre-Processor, 2004

[32] Victor Andrei: Monitoring the Cable Test Runs, April 2006

[33] Björn Gosdzik: First comparison of Trigger and Detector data, Level-1 Calorimeter Trigger Joint Meeting, November 2006

[34] Kambiz Mahboubi, Rainer Stamen, Florian Föhlisch and Victor Andrei, private discussion and email correspondence

List of Figures

List of Tables

Glossary

ASIC	Application Specific Integrated Circuit
BCID	Bunch-Crossing IDentification
CASTOR	CERN Advanced STORage manager
CIS	Charge Injection System
CMT	Configuration Management Tool
CP	Cluster Processor
CSC	Cathode Strip Chamber
CS	Central Solenoid
CTP	Central Trigger Processor
CVS	Concurrent Versions System
DAC	Digital-to-Analogue Converter
DAQ	Data Acquisition
EC	Electromagnetic Calorimeter
ECT	End-Cap Toroids
EF	Event Filter
FADC	Flash Analogue-to-Digital Converter
FCAL	Forward Calorimeter
FIFO	First In - First Out
FIR	Finite Impulse Response. A type of digital filter
FWHM	Full-Width at Half-Maximum. A measure of the width of a signal
HEC	Hadronic End-Cap
HLT	High Level Trigger
ID	Inner Detector
JEP	Jet/Energy-sum Processor

LAr	Liquid Argon
LCD	LVDS Cable Driver
LEP	Large Electron Positron Collider
LHC	Large Hadron Collider
LUT	LookUp Table
LVDS	Low-Voltage Differential Signaling
LVL1	Level-1 Trigger System
LVL2	Level-2 Trigger System
MCM	Multi-Chip-Module
MDT	Monitored Drift Tubes
MSSM	Minimal-Super-Symmetric-Standard Model
OH	Online Histogramming server
PCB	Printed-Circuit Board
PMT	Photomultiplier Tube
POOL	Pool Of persistent Objects for LHC (Data management)
PPr	Pre-Processor
ReM_FPGA	Readout Merger Field Programmable Gate Array
RGTM	Rear G-Link Transmission Module
ROB	ReadOut Buffer
ROD	ReadOut Driver module
SCT	SemiConductor Tracker
SM	Standard Model
TCM	Timing and Controll Module
TileCal	Tile Calorimeter
TRT	Transition Radiation Tracker
TTCdec	TTC Decoder
TTC	Timing, Trigger and Control
VME	Versa Module Euro
WLS	WaveLengthShifting fibres

Acknowlegdement

I wish to express my gratitude to everybody who helped me with or contributed to this thesis in any way. My special thanks go to:

- Prof. Dr. Karlheinz Meier for giving me the opportunity to do this thesis at the ATLAS group at the Kirchhoff-Institut für Physik and at CERN
- Prof. Dr. Ulrich Uwer for spending his time to be my second corrector
- Dr. Paul Hanke for answering all my questions and his help to understand the PPr system in his colorful manner
- Dr. Kambiz Mahboubi for his tireless support mainly during my CERN time
- Dr. Rainer Stamen for his enthusiasm and all the fruitful discussions
- My colleagues Victor Andrei, Frederik Rühr, Florian Föhlisch and Pavel Weber for many discussions and their willingness to answer all my questions
- Verena Pohl for her stringently proofreading
- All my friends in Heidelberg for the wonderfull time outside the university

And finally to my parents Edeltraud and Peter and my brother Marco. They gave me always a great moral support especially in hard times and they supported me in many other ways.